

**NBSIR 77-1232 (ERDA)**

# **Development of In-Situ Techniques for the Detection and Measurement of Corrosion of Copper Concentric Neutrals in Underground Environments**

---

RECEIVED

JATE 4/19/77  
OTP

J. Kruger, U. Bertocci, E. Escalante, and J. L. Mullen

Corrosion and Electrodeposition Section  
Metallurgy Division  
Institute for Materials Research  
National Bureau of Standards  
Washington, D. C. 20234

April 1977

Annual Report

Prepared for  
Energy Research and Development Administration  
Washington, D. C. 20545



NBSIR 77-1232 (ERDA)

**DEVELOPMENT OF IN-SITU  
TECHNIQUES FOR THE DETECTION  
AND MEASUREMENT OF CORROSION  
OF COPPER CONCENTRIC NEUTRALS  
IN UNDERGROUND ENVIRONMENTS**

---

J. Kruger, U. Bertocci, E. Escalante, and J. L. Mullen

Corrosion and Electrodeposition Section  
Metallurgy Division  
Institute for Materials Research  
National Bureau of Standards  
Washington, D. C. 20234

April 1977

Annual Report

DISTRIBUTION OF THIS DOCUMENT IS UNLIMITED

Prepared for  
Energy Research and Development Administration  
Washington, D. C. 20545



---

**U.S. DEPARTMENT OF COMMERCE, Juanita M. Kreps, *Secretary***

**Dr. Betsy Ancker-Johnson, *Assistant Secretary for Science and Technology***

**NATIONAL BUREAU OF STANDARDS, Ernest Ambler, *Acting Director***



Development of IN-SITU Techniques for the Detection and Measurement  
of Corrosion of Copper Concentric Neutrals in Underground Environments

Annual Technical Report for Period January 15, 1976 to January 15, 1977

J. Kruger, U. Bertocci, E. Escalante, and J. L. Mullen

1. Introduction

2. Laboratory Experiments

2.1 Corrosion Tests

2.1.1 Experimental Conditions

2.1.2 Experimental Results

2.1.3 Examination of the Results

2.1.3.1 Effect of Solution Composition and Atmosphere

2.1.3.2 Effect of Convective Motion

2.1.3.3. Effect of a.c.

2.1.3.4. Effect of Coupling with CPE

2.2 Current-Potential Measurements

2.2.1 Potentiodynamic Scans

2.2.2 Long-Term Current-Potential Data

2.3 Chemical Analysis of the Surface

2.4 Noise Measurements

2.5 Discussion of the Laboratory Experiments

3. Field Experiments

3.1 Material Selection and Specimen Design

3.2 Experimental Procedure

3.3 Results and Discussion

3.4 Summary of the Field Experiments

4. Plans for Future Work

5. Executive Summary

# Development of IN-SITU Techniques for the Detection and Measurement of Corrosion of Copper Concentric Neutrals in Underground Environments

Annual Technical Report for Period January 15, 1976 to January 15, 1977

J. Kruger, U. Bertocci, E. Escalante, and J. L. Mullen

## 1. Introduction

This is the first annual report of a three-year project, whose objective is to develop techniques and instrumentation for detecting and measuring the extent of corrosion of the copper concentric neutral (CCN) wires of buried electric cables without removal of the cables from the soil. By being able to locate the sites where the rate of corrosion is high, preventive measures such as altering the environment (e.g., by backfilling with different soils), application of cathodic protection, or other yet to be determined ways, can be applied.

The approach to this problem consists in finding first, by means of laboratory tests, the conditions that promote a high corrosion rate, and subsequently to create those conditions on buried cables in order to compare laboratory and field results.

Measurement methods such as the recording of polarization curves and electrode potential are to be evaluated with respect to their ability to detect and measure corrosion of buried cables. Also, at the same time, other proposed methods, such as a.c. impedance and electrochemical noise measurements, would first be developed in the laboratory and subsequently, if found promising, field-tested.

The measurement techniques eventually will be applied in the field to corroding and non-corroding cables, and then potential for detecting corrosion assessed.

A major effort of the first year's work was directed at finding, by means of laboratory experiments, which conditions favor the onset of the rapid, localized corrosion that it is the aim of the project to detect in the field. Also, development of new measurement techniques has been initiated.

In the field, burial of the cable and related materials as well as all necessary electrical connections were completed, and systematic measurements on the underground specimens were initiated.

## 2. Laboratory Experiments

### 2.1 Corrosion Tests

#### 2.1.1 Experimental Conditions

A number of specimens of copper concentric neutral (CCN) wire made of tinned copper underwent long term corrosion tests for times of order of 2000 h.

# Development of IN-SITU Techniques for the Detection and Measurement of Corrosion of Copper Concentric Neutrals in Underground Environments

Annual Technical Report for Period January 15, 1976 to January 15, 1977

J. Kruger, U. Bertocci, E. Escalante, and J. L. Mullen

## 1. Introduction

This is the first annual report of a three-year project, whose objective is to develop techniques and instrumentation for detecting and measuring the extent of corrosion of the copper concentric neutral (CCN) wires of buried electric cables without removal of the cables from the soil. By being able to locate the sites where the rate of corrosion is high, preventive measures such as altering the environment (e.g., by backfilling with different soils), application of cathodic protection, or other yet to be determined ways, can be applied.

The approach to this problem consists in finding first, by means of laboratory tests, the conditions that promote a high corrosion rate, and subsequently to create those conditions on buried cables in order to compare laboratory and field results.

Measurement methods such as the recording of polarization curves and electrode potential are to be evaluated with respect to their ability to detect and measure corrosion of buried cables. Also, at the same time, other proposed methods, such as a.c. impedance and electrochemical noise measurements, would first be developed in the laboratory and subsequently, if found promising, field-tested. The measurement techniques eventually will be applied in the field to corroding and non-corroding cables, and then potential for detecting corrosion assessed.

A major effort of the first year's work was directed at finding, by means of laboratory experiments, which conditions favor the onset of the rapid, localized corrosion that it is the aim of the project to detect in the field. Also, development of new measurement techniques has been initiated.

In the field, burial of the cable and related materials as well as all necessary electrical connections were completed, and systematic measurements on the underground specimens were initiated.

## 2. Laboratory Experiments

### 2.1 Corrosion Tests

#### 2.1.1 Experimental Conditions

A number of specimens of copper concentric neutral (CCN) wire made of tinned copper underwent long term corrosion tests for times of order of 2000 h.

Several environmental variables were tested for their influence on corrosion susceptibility. They were:

a) Composition of the electrolytic solution. Four solution compositions were extensively tested: 2%  $\text{Na}_2\text{SO}_4$ , 2%  $\text{Na}_2\text{SO}_4$  + 1%  $\text{NaCl}$ , 0.42 M  $\text{NaClO}_4$  and 0.42 M  $\text{NaClO}_4$  + 1%  $\text{NaCl}$ . The pH of all solutions was approximately neutral. These solution compositions were chosen so as to test the influence of two salts, sulfate and perchlorate, thought not to be particularly aggressive, both in the presence and in the absence of chloride ions, which are supposed to be corrosive in the soil.

b) Composition of the gaseous atmosphere in contact with the solution. Both an oxygen and a nitrogen atmosphere were tested, the latter representing poor soil aeration.

c) Convective motion in solution. Since in the soil convective transport is negligible compared with a liquid, some corrosion tests were carried out in 1% Agar gel, with the solution having the same compositions given in a) in order to simulate soil conditions.

d) Superimposed a.c. signal. In order to investigate the effect of a.c. current flowing between the wire and the soil, tests were performed where a 60 Hz a.c. signal was applied between the test specimen and a large surface area counterelectrode. In order to approximate a potentiostatic condition without entailing the use of a potentiostat for each test cell, a circuit scheme such as that of Fig. 1 was used. The resistance  $R$  is used to measure the current, and the capacitor  $C$  is inserted to prevent circulation of a d.c. current. In order to approximate a potentiostatic behavior, the voltage  $V$  supplied by the variable transformer should be as close as possible to the voltage between the electrode under study  $E$  and the solution in its immediate vicinity. In other words, all other voltage drops in the circuit should be as small as possible. In the practical case the resistance  $R$  was chosen as  $10 \Omega$ , and the capacitance was made by two  $220 \mu\text{F}$  electrolytic capacitors put in series so as to block all d.c. components. In separate experiments it was found that the d.c. resistance of the two capacitors at low voltages is greater than  $1 \text{ G} \Omega$ . The impedance of the two capacitors is of the order of  $24 \Omega$  at 60 Hz. The counterelectrode  $CE$  is made of a stainless steel sheet of large surface area ( $75 \text{ cm}^2$  compared with about  $2 \text{ cm}^2$  for the working electrode). In a number of experiments it was found that 60 to 80% of the total impedance was found between  $E$  and the adjacent solution (the measurement was carried out by means of a third electrode inserted in the cell).

Here are two examples of how the voltage drop is distributed:

Cu in 2% Na<sub>2</sub>SO<sub>4</sub>

Tinned Cu in 2% Na<sub>2</sub>SO<sub>4</sub>

A=5 cm<sup>2</sup>, c.d.=0.447 mA/cm<sup>2</sup>

A=2.2 cm<sup>2</sup> c.d.=0.215 mA/cm<sup>2</sup>

Voltage drop, mV	$\phi=0^\circ$	$\phi=90^\circ$	$ Z , \Omega$	$\phi=0^\circ$	$\phi=90^\circ$	$ Z , \Omega$
Total	146	97	78.4	71	82	229
R	- 1.5	22.3	10.0	- 1.5	4.5	10.0
C	53	4.75	23.8	10.5	4.0	23.7
CE	6.5	9.5	5.15	1.0	1.8	4.34
E	87	63	48.1	61	71	197
$ Z _E /  Z _T, \%$			61			86

Fig. 2 shows voltage and current signal for the cell whose data are in Col. 1. The distortion of the current signal from a sinusoidal one is considerable.

With such a circuit the cell voltage and current density could not be maintained as constant and have varied between 150 and 450 mV and 1 and 8 mA/cm<sup>2</sup>, respectively. In the tables that summarize our results, an a.c. resistance has been reported, calculated as the ratio between the average cell voltage and the electrode current density. This number is an indication of the ease for the a.c. to flow between the wire and the solution. A smaller resistance, therefore, entails a larger current density, and vice versa.

e) Coupling with conducting polyethylene (CPE). The outer part of the insulating sheath of the cable is covered with CPE, formed by carbon powder embedded in polyethylene, which is in electric contact with the neutral wire. Since the open circuit potential of CPE tends to be fairly positive, as shown in Fig. 16, the effect of coupling the CCN wire with CPE was also examined. In these experiments the short circuit current flowing between CCN wire and CPE was periodically measured by inserting a current-to-voltage converter between the two. Since the internal resistance of the instrument is effectively zero, it was possible to measure the short circuit current without affecting its magnitude.

### 2.1.2 Experimental Results

The results obtained from the corrosion tests are presented as follows: Figs. 3, 4, 5, and 6 give the potential of the tinned CCN wire vs. SCE in solutions containing Na<sub>2</sub>SO<sub>4</sub> with and without NaCl and under an O<sub>2</sub> or N<sub>2</sub> atmosphere. Figs. 7, 8, 9, and 10 are the analogous graphs for solutions containing NaClO<sub>4</sub>. Also, Tables I-VIII summarize the results by giving average values of the electrode potential, of the a.c. resistance and of the short circuit current density between specimen and CPE when appropriate, as well as a description of the appearance of the wire after the test as obtained by visual inspection.

under a low power microscope. Finally, Figs. 11, 12, 13, 14, and 15 show some color photographs of the wires after the test.

### 2.1.3 Examination of the Results

#### 2.1.3.1 Effect of Solution Composition and Atmosphere

Under a nitrogen atmosphere the rate of corrosion is slower than in the presence of oxygen. The electrode potentials, as a consequence, tend to be more negative; if the tinning coat is continuous, the potential can remain at low voltages, -400 to -500 vs. SCE for fairly long periods of time, as it had been found in preliminary experiments. The tinning coat on the CCN wire in use now always presents many small flaws, and very low potentials have never been maintained for long times. The steady state values obtained on this wire (see Figs. 3, 4, 7, and 8) are higher in the absence of  $\text{Cl}^-$  ions (about 0 mV in  $\text{NaClO}_4$  and -50 in  $\text{Na}_2\text{SO}_4$ ) than in their presence (from -130 to -220 mV in  $\text{Na}_2\text{SO}_4$  and from -100 to -200 mV in  $\text{NaClO}_4$ ). Potentials are shifted towards more positive values by oxygen, and they are higher in the absence of chlorides, where  $\text{NaClO}_4$  solutions show, as in  $\text{N}_2$ , higher values (+40 to 80 mV) than  $\text{Na}_2\text{SO}_4$  solutions (from 0 to +30 mV). When chlorides are present, the differences are much less pronounced, also because the spread is larger. In sulfate, the potential ranges from +30 to -60 mV and in perchlorate from +50 to -80 mV, with the solutions containing agar showing the lowest values because of the lower availability of oxygen.

The a.c. resistance shows a definite tendency towards lower values in nitrogen than in oxygen. Chloride in solution has the effect of decreasing even more the resistance of the electrode. If these findings are compared with the results of the visual inspection of the wires after the test, it is clear that a high a.c. resistance is associated with and probably caused by extensive scale formation. Low resistance specimens in general look only slightly corroded. Chlorides, on the other hand, promote corrosion but evidently contribute to the formation of more conductive reaction products than those formed in their absence.

Comparison of the specimens kept in sulfate and perchlorate solutions show that, all other conditions being equal, the extent of corrosion is greater in perchlorate. In particular the tinning coat can be removed more easily in a number of cases (see Figs. 13 e) and f)), from wires tested in  $\text{NaClO}_4$ .

#### 2.1.3.2 Effect of Convective Motion

Preliminary experiments had shown that corrosion in agar under a  $\text{N}_2$  atmosphere was very small, and, therefore, it had been decided to examine the effect of preventing convective motion only under oxygen. Corrosion was found to be rather small in the absence of chlorides although some pit initiation was detected. In solutions containing chlorides, however, extensive pitting was found towards the bottom of the wire, with a pattern suggesting differential aeration. This was true both in sulfate (see Fig. 12a) and perchlorate (see Figs. 14 e) and f) and Fig. 15 f)).

### 2.1.3.3 Effect of a.c.

The superposition of an a.c. signal did not have a clear effect on the electrode potential but has definitely enhanced the corrosion of the wire. In particular, pitting as opposed to a more uniform attack, has been detected almost exclusively on specimens tested with a.c. Even for the tests in the milder  $N_2$  atmosphere, corrosion and pitting could be found (see, for instance, Figs. 14 a) and b)). It must be kept in mind that a.c. current in  $N_2$  atmosphere was often much larger than under oxygen, as discussed in 2.1.3.1, and this may have enhanced the effect of a.c. On the other hand, in  $O_2$  a smaller current did not prevent the enhancement of the attack and pit formation.

### 2.1.3.4 Effect of Coupling with CPE

Since the potential of CPE is more positive than that of the CCN wire, as shown in Fig. 16, it was expected that coupling between CPE and wire would shift the potential toward more positive values and that an anodic short circuit would flow in the electrolyte from the wire to the CPE. These expectations have been largely fulfilled. In nitrogen the electrode potentials of the wires coupled to CPE almost without exception are 20 to 100 mV more positive than the corresponding wires tested without coupling. In oxygen the situation is less clear, but wires coupled to CPE tend to be more positive.

As far as the direction of the short circuit current is concerned, a few exceptions have been found where a cathodic current, always very small, was measured. There is no simple explanation for it. It is possible that the reversal was caused by transport of some of the corrosion products to the CPE, providing an anodic reaction there. This explanation is suggested by the fact that some Cu products have been found on the CPE and also that in the corresponding tests in agar, where such a transport could not occur, the short circuit current was anodic on the wire.

Coupling to CPE increased somewhat the rate of attack of the wires: under  $N_2$ , attack occurred under the tinning coat so that often it could be removed by gentle scratching or even by brushing with a soft brush (see, for instance, Figs. 13 e) and f)). Cases where there was attack under the tinning were associated with relatively high short circuit current densities, that is larger than  $1 \mu A/cm^2$  and up to  $6 \mu A/cm^2$  in one instance. In general, however, this attack was not associated with pit formation.

The short circuit current density is influenced by both the availability of oxygen that shifts the potential in a positive direction and by the formation of a resistive layer on the wire as indicated by the a.c. resistance. The two factors work against each other, but the second seems to be more important. Therefore, short currents in  $N_2$  atmosphere were often larger than in  $O_2$  in spite of the fact that the potential was more than 100 mV higher in the latter condition.

## 2.2 Current-potential Measurements

### 2.2.1 Potentiodynamic Scans

Potentiodynamic scans afford a useful way to examine quickly the main features of the current-potential behavior of an electrode. For this reason, scans on CCN wire were taken in  $\text{Na}_2\text{SO}_4$ , both in the presence and in the absence of  $\text{NaCl}$ . The results, given in Figs. 17 and 18, show a number of peaks, with a very large one in  $\text{NaCl}$  at about  $-150$  mV vs. SCE. The wires showed loss of the tinning coat during the measurements, and in order to clarify the contribution of copper and of the tinning coat to the electrochemical behavior, potentiodynamic scans were taken both on pure copper and on a piece of alloy having the same composition, about 90% Pb and 10% Sn, of the tinning bath used by the manufacturer of the cable.

The results obtained on pure copper are shown in Figs. 19 to 24. In the absence of chlorides no detectable formation of a passive, protecting film is observed, whether in  $\text{Na}_2\text{SO}_4$  or in  $\text{NaClO}_4$ . Fig. 19 shows the scans in sulfate in oxygen or in nitrogen over the scan range of greatest interest for our study from  $-800$  to  $+200$  mV vs. SCE. Fig. 20 shows the monotonic increase of anodic current with the extension of the range up to  $+800$  mV. The curve in Fig. 21 shows that the same behavior, with even larger current densities, is observed in perchlorate. From these data, and from visual observation of the solution in the cell, it is quite clear that the  $\text{Cu}^{++}$  ion produced anodically is precipitated as hydroxide away from the electrode surface and never forms any protective layer on the metal surface. As a consequence, no cathodic reduction takes place, in the absence of oxygen, until hydrogen can evolve during the cathodic sweep.

In the presence of chlorides in solution, a precipitate is formed during anodic attack, sufficiently adherent to produce a cathodic peak during the negative sweep. However, the precipitate is very ineffective in protecting the metal, and although causing some poorly reproducible peaks and inflections on the anodic branch, it fails to limit the anodic current density which can reach  $60 \text{ mA/cm}^2$  at  $+800$  mV as shown in Fig. 23. Comparison between Figs. 22, 23, and 24 shows that the position of the cathodic peak is shifted toward more negative values by extending the anodic range as well by increasing the scan rate. The anodic branch, on the contrary, is little affected by changes in scan rate indicating that the behavior is not a transient one.

The electrochemical behavior of the 90% Pb-10% Sn alloy, both in the absence and in the presence of chlorides, is described in Figs. 25, 26, and 27. Scans were carried out changing the range and the rate in chloride containing solutions. The results have confirmed that the more negative of the cathodic peaks corresponds to the anodic peak and is caused by the irreversible reduction of a  $\text{PbSO}_4$  film. The more positive of the cathodic peaks is absent if the scan does not exceed  $-200$  mV (see dashed curve in Fig. 27) and corresponds to an anodic oxidation occurring between  $-200$  mV and  $+200$  mV, probably the formation of lead chloride. The metal exhibits passive behavior up to  $800$  mV vs. SCE.

The results show, at least qualitatively, that some of the features seen on the potentiodynamic scan on tinned wire (Figs. 17 and 18) are indeed due to the tinning coat. However, it must be kept in mind that the alloy used in these experiments does not correspond to the composition of the tinning coat as discussed in Section 2.3.

### 2.2.2 Long-Term Current-Potential Data

The current-potential data described in the preceding section have been obtained from freshly prepared samples where no accumulation of corrosion products has taken place. In order to monitor the change in electrochemical behavior with time of exposure of the CCN wires to the environment for a better correlation with the field measurements, cells similar to those used for the corrosion tests but with provision for applying current and recording the potential have been set up. The data are being taken at intervals of the order of a month. The measurements are done potentiostatically, shifting the potential by small increments from the open circuit potential, and waiting several minutes for every point in order to stabilize the current.

Values obtained in December 1976 are shown in Fig. 28 and those obtained in January 1977 in Fig. 29. For the moment the open circuit potentials have shifted somewhat, but there are not significant changes in the curves. The corrosion current densities, estimated roughly from the curves, are of the order of  $1 \mu\text{A}/\text{cm}^2$ .

### 2.3 Chemical Analysis of the Surface

In order to determine the extent of removal of the tinning coat during corrosion tests, some specimens have been analyzed in a scanning electron microscope using energy dispersive x-ray detection.

In Fig. 30 are the spectra of an untouched tinned wire as well as comparison spectra of copper and two compositions of Pb-Sn alloy. It is evident that on the tinned wire the Sn/Pb ratio is larger than in either one Pb-Sn alloy tested, 90% Pb-10% Sn being the composition of the tinning bath. The tinning layer, therefore, consists mainly of Sn with probably only 20 to 30% Pb. This is not surprising, since Sn forms intermetallic compounds with Cu, and it is taken up preferentially during the tinning process. Figs. 31 and 32 show spectra of corroded specimens, all of them after tests in sulfate solutions. Spectrum 31 a) was taken on specimen #1 (see Table III) where the surface was covered with a  $\text{Cu}_2\text{O}$  layer. No tinning was detected, although the tinning coat was still present in some areas. Spectrum 31 b) was taken on specimen #101 (see Table I). The only effect of the corrosion tests was some loss of Pb on the surface. Spectrum 31 c) was taken on specimen #5 (see Table III), exposed to conditions quite similar to 31 a), except that it was coupled with CPE. Its potential tended to be about 100 mV more positive than 31 a) throughout the tests. The analysis results show a significant amount of Sn still present as well as formation of  $\text{PbCl}_2$ , indicated by the presence of a small Cl peak. The tinning is still largely present on 31 d) (specimen #104, see Table III) where no a.c. was applied. Also no Cl peak can be seen. The wire whose

analysis is shown in Fig. 32 (#119, see Table VII) was exposed in agar to an oxygenated solution containing chlorides. The Sn has disappeared, but both Pb and Cl are visible. It is likely that because of lack of convection, in spite of the thorough attack of the tinning coat, the  $PbCl_2$  formed remained on the surface.

## 2.4 Noise Measurements

In our proposal, we have mentioned that the detection and analysis of voltage fluctuations will be tested as a possible means of finding areas of high corrosion rate in the field. The amplitude and the frequency of the noise generated by corroding metals has been shown in some cases to be correlated with the corrosion rate or to change in a significant way above and below the pitting potential. The method is, however, a novel one, and a large amount of preliminary laboratory work is expected before the method can be field-tested.

During this year the equipment necessary for the measurement of noise by two methods has been assembled and tested. The first method is essentially based on using a spectrum analyzer. The schematic circuit is shown in Fig. 33. In this method the potential of the electrode is varied by applying a constant current. However, it would be better if the noise measurements could be carried out under potentiostatic conditions. For this purpose, a special low noise potentiostat is being developed and built at N&S and should shortly be ready for testing.

Preliminary measurements of the noise of electrochemical systems has been carried out in order to examine the capabilities and limitations of the system. Fig. 34 shows two spectra for electrode systems that are expected to have a low noise. The lower spectrum coincides essentially with the background instrumental noise.

Some measurements have been carried out on an iron electrode in a solution where pitting can occur. Under anodic polarization a significant increase of the noise was observed when the electrode potential was above the pitting potential. Fig. 35 shows the spectra obtained at different potentials, and Fig. 36 shows the time recordings of the electrode potential above and below the pitting potential.

The second method for noise measurements is supposed to allow the measurement of a source lower than the noise level of the electronic equipment employed. The method consists in sending the noise signal to be measured on two parallel amplifying and filtering channels as shown in Fig. 37. The output signals of the two channels are fed to a multiplying amplifier with averaging capability. Each channel signal is the sum of the source noise and of the instrument noise, but since the instrument noise is uncorrelated, the average of its product is zero, and the output of the multiplying amplifier should be only the square of the source noise.

Fig. 30 shows some results of preliminary tests. On it is reported the instrument noise as well as the noise generated by a 10 K $\Omega$  resistor. At high frequencies, the thermal noise of the resistor is, as expected, higher than the instrumental noise. The larger peak is caused by some 60 Hz pickup, but from approximately 10 Hz down, the noise is lower than the instrument noise. This method is expected to be usable above 0.2 Hz.

## 2.5 Discussion of the Laboratory Experiments

The results obtained from the long exposure time corrosion tests give useful guidelines on ways to artificially cause corrosion in buried cables. It is evident that the application of an a.c. signal is a powerful means to cause pitting. However, a.c. is probably not absolutely necessary, as shown by some cases when extensive corrosion occurred without it, but causes a considerable increase in the rate of attack.

The presence of a reducible species such as oxygen was expected to enhance corrosive attack, and this has been verified experimentally to a certain extent. However, the effect of the attack is the formation of layer of reaction products that can slow down considerably further corrosion. Which of the two effects of the availability of oxygen, thermodynamic factors favorable to corrosion or kinetic factors opposed to it, will be predominant in a certain instance may depend on subtle differences in the environment and may be difficult to predict.

The presence or absence of a protective scale influences the amount of a.c. leakage and probably explains why extensive pitting was found in tests where oxygen was kept low by a nitrogen blanket; in these conditions, no protective scale was found, and extensive pitting occurred in many cases. Analogous conclusions can be drawn from those tests in agar where oxygen could not readily reach the bottom part of the specimen, and the attack there was quite severe. These tests also point to differential aeration as a possible cause of failure in the field.

The addition of chloride ions also enhances corrosive attack, since they tend to reduce the resistance of the protective layer.

A few months ago it was pointed out by Dr. Nesslage of Phelps-Dodge, that sulfates, or perhaps other sulphur-containing materials, may play an important role in the corrosion of CCN wire in the field. To examine this possibility, corrosion tests employing NaClO<sub>4</sub> instead of Na<sub>2</sub>SO<sub>4</sub> as the main electrolyte were carried out. From the results reported here it appears that no special role is played by sulfates in the laboratory tests. Although the effect is quite minor, the NaClO<sub>4</sub> solutions seem to be a slightly more corrosive environment than Na<sub>2</sub>SO<sub>4</sub>, perhaps because all perchlorates of the heavy metals (including Pb) are more soluble than the corresponding sulfates.

The crude measurements of the electrode impedance obtained by monitoring the a.c. voltage and current have given some interesting clues concerning the susceptibility of the CCN wire to undergo rapid attack. This seems to be an encouraging result that may point to a.c. impedance measurements as a useful diagnostic tool. It is our intention to start soon more extensive measurements of the impedance at various frequencies with the aim of developing it as a field measurement method.

### 3. Field Experiments

#### 3.1 Material Selection and Specimen Design

Considerable time and effort was spent in trying to determine whether any particular cable design or combination of cable components was more susceptible to corrosion deterioration than others and, therefore, better suited for field testing. This search developed inconclusive information since apparently failures due to corrosion have occurred in all designs and component combinations. It was then decided that we adopt the underground cable design that is most widely used. The following specifications were finally accepted.

#2 AWG stranded aluminum conductor in cross-linked, thermosetting polyethylene insulation with ten strands of #14 AWG coated copper concentric neutral wires manufactured within AEIC #5 and IPCEA S-61-402 specifications.

1100 feet of cable were ordered from the Reynolds Metals Company. A significant reason for placing this order with Reynolds was that they supplied a bulk sample of the coating alloy and over one hundred meters (300 ft.) of bare copper wire.

The cable was cut to desired lengths but otherwise used as received. For the field study, cable lengths of 15 meters (~ 45 ft.) were used. An insulated conductor was attached midway between the two ends of the cable and, once buried, extended above ground to a terminal block.

The cable components (i.e., bare or coated copper wire, coating alloy, carbon impregnated plastic) were handled in the following way. One meter (39 inches) length sections of cable were cut with cable shears. The coated CCN wires were removed from these sections and soldered together as shown in Fig. 39a. Each specimen had an insulated electrical lead attached to it which extended above ground after burial. All solder joints were coated with silicon rubber adhesive to avoid undesirable galvanic effects.

Similarly the bare copper wire was cut to a length equivalent to one meter (39 inches) of cable and assembled as shown in Fig. 39 b.

The one meter length of cable component that remained after the CCN wires were removed had the conducting polyethylene (CPE) film on the outside. The ends of these pieces of cable were sealed with silicon rubber adhesive. Electrical contact was made to the CPE by tightly wrapping bare wire around its circumference at a point midway between the two ends as shown in Fig. 40 a. This binding was also coated with silicon rubber adhesive.

The resistivity of the CPE was measured to be  $55 \Omega \text{ cm}$ . It was observed that mechanical flexing during handling increased the resistivity of the CPE by as much as a factor of two in an irreversible way.

The 90% lead (Pb) 10% tin (Sn) coating alloy ingot was cold rolled into sheet with a thickness of 0.5 mm (0.02 inches). Specimens cut from this sheet were such that their total surface area equaled the surface area of the CCN wires on a meter (39 inches) length of cable. Fig. 40 b illustrates the geometry of this specimen whose total surface area is 512 cm<sup>2</sup>. In addition, the alloy was spectrographically analyzed. Other than Pb and Sn, the total sum of other constituents is less than 2%. Neither of the two major impurities, antimony (Sb) and copper (Cu), form intermetallics with lead as indicated by their phase diagrams.

### 3.2 Experimental Procedure

The field specimens were buried at our NBS site in November 1976. The burial plan is illustrated in Fig. 41.

Four trenches each approximately 0.6 m (25 in.) wide, 1 m (3 ft.) deep and from 17 to 30 m (50 to 90 ft.) long were dug with a back hoe. Three of these trenches hold the 15 m (45 ft.) cables as shown. The first of these three trenches contains the cables with the superimposed alternating current (AC). The current density on the CCN wires of these cables is 1 mA/cm<sup>2</sup>. The fourth, and longest trench, contains the cable components which are buried alone or galvanically coupled to another component.

Corrosion data has been gathered in the field by electrochemical techniques initially at intervals of two weeks. These preliminary measurements consisted of potential measurements of all specimens, galvanic current measurements of all coupled specimens, and corrosion rate measurements of the 15 m (45 ft.) cables and the noncoupled components.

Potential measurements were made using a high input impedance ( $10^{14}$  ohm) voltmeter and a Cu-CuSO<sub>4</sub> reference electrode.

The galvanic current measurements on the cable components were made with a zero input impedance ammeter. This measurement indicates not only the amount of current flowing, and, thus, the amount of metal dissolution resulting between two components, but also its direction of flow so that the anode-cathode relationship can be identified.

Corrosion rate measurements were made by conventional polarization methods. Up to this time only the linear polarization technique has been used. In this case the potential of the specimen is polarized by not more than 10 mV in the cathodic (active) direction and the current required to do this noted. The Stern-Geary equation (1) is used as follows:

$$\frac{\Delta E}{\Delta I} = \frac{1}{2.3 I_{CORR}} \left[ \frac{B_a B_c}{B_a + B_c} \right]$$

In this equation  $\Delta E$  is the overvoltage of the corroding electrode produced by the polarizing current  $\Delta I$ ;  $B_a$  and  $B_c$  are the slopes of the anodic and cathodic polarization curves, respectively, in the Tafel region, and  $I_{CORR}$  is the corrosion current. The constants  $B_a$  and  $B_c$  are both assumed to be equal to 0.1 in this equation. This assumption results in the following equation:

$$I_{CORR}(mA) = \frac{21.7 \Delta I (mA)}{\Delta E (mV)}$$

Through the use of this equation the corrosion rate is then calculated.

The counterelectrode was a rod driven into the ground some 15 or 20 m (45 or 55 ft.) from the specimens. Likewise, the reference electrode was 15 or 20 m (45 or 55 ft.) on the opposite side of the specimens. IR-DROP compensation was necessary.

### 3.3 Results and Discussion

The field study is a relatively long term program in that once the specimens are buried, they will remain in the ground from one to three years. During this time, as has already been described, electrochemical measurements will be carried in situ on the specimens. Since the specimens have only been in the ground about ten weeks, the data presented here are very preliminary in nature and subject to change.

Previous experience has shown that settling of the soil continues for several weeks after burial. During this settling period, electrochemical data tend to be unstable.

The potential measurement data collected during the first ten weeks and listed in Table 9, for example, show a general shift in a negative (active) direction. The potentials appear to be approaching some equilibrium level with time.

The specimens listed in Table 9 are separated into three groups. The first group is the uncoupled cable components. The second group is the galvanically coupled cable components. The last group is the 15 m (45 ft.) cables with or without imposed alternating current.

The galvanic currents listed in group 2 show some general tendencies. In practically every case the conducting polyethylene (CPE) is cathodic to the other materials. That is, it causes the metal to which it is connected to corrode. The larger the galvanic current the greater is the rate of reaction. One can see that the lead-tin coating alloy sheet (CAS) is corroding about ten times faster than the bare copper wire (BCW) or the coated copper wire (CCW). In the case where the BCW is connected to the CAS, the CAS is acting as the anode and, hence, corroding. This in turn is cathodically protecting the copper wire.

The corrosion rate measurements made on the uncoupled cable components after forty days of burial indicate that the bare copper wire is corroding at a rate of less than 1 mdd\*. The coated copper wire during the same time period is deteriorating at a rate that is four times greater or 3.7 mdd. The corrosion rate of the coating alloy is only slightly less at 2.5 mdd.

3.4 Summary of the Field Studies

1) The field study specimens have now been in the ground for over ten weeks.

2) Potential measurements indicate that settling of the soil is just beginning to stabilize.

3) The galvanic current measurements reveal that 90% lead-10% tin coating alloy is cathodically protecting the copper wire. These measurements also show that when the conducting polyethylene is galvanically connected to the bare copper wire, the coated wire, or the coating alloy, they are sacrificially corroded.

4) After forty days of burial the polarization data of the cable components show that the corrosion rate of the bare copper wire is less than 1 mdd, and the corrosion rate of the coated copper wire and the coating alloy is two to four times greater.

4. Plans for Future Work

During the next year of this project, the following work is planned:

<u>Activity</u>	<u>Expected Completion</u>
Introduce corrosive conditions identified in the laboratory to the field studies in order to make measurements under corrosive conditions	3 months
Complete examination by retrieval of 6 months exposed cables	6 months
Complete evaluation of polarization and potential techniques in field	9 months
Complete examination in laboratory of AC and noise techniques	10 months
Start adoption of laboratory developed techniques to field tests	12 months
Complete examination by retrieval of one year exposed cables	12 months

\*mg/dm<sup>2</sup>/day

## 5. Executive Summary

The first year's work of a three-year project aimed at developing techniques and instrumentation for detecting and measuring corrosion in buried copper concentric neutral (CCN) wires has been completed.

Laboratory corrosion tests and electrochemical measurements have given information on which environmental conditions are likely to cause corrosion similar to that of concern in the field. This knowledge is necessary in order to be able to cause corrosion at will in buried CCN wires used to test detection and measurement techniques. Presence of chlorides, availability of oxygen and a.c. leakage from wires to the electrolyte are the major factors in causing rapid corrosion. Preliminary examinations of polarization as impedance and corrosion "noise" in the laboratory were initiated.

A field test site has been set up, and a number of cables buried. Polarization and potential measurements on these specimens to provide base line data were initiated.

Milestones for the coming year were set involving: a) application of the first year results to provide corroding systems for field testing of detection techniques; b) testing of new detection and measuring techniques in the laboratory; and c) two retrievals and examinations of buried cables.

## REFERENCES

- (1) M. Stern and A.L. Geary, J. Electrochem. Soc., 104 (1), 56 (1957).

TABLE I Solution:  $\text{Na}_2\text{SO}_4 \cdot \text{N}_2$  Atmosphere

N	CPE	a.c.	Agar	d.c. V, mV	a.c. R, $\Omega \cdot \text{cm}^2$	s.c. c.d., $\mu\text{A}/\text{cm}^2$	Photo #	Visual Observation
3		*		$-50 \pm 20$	180			$\text{Cu}_2\text{O}$ layer, tin coat excellent underneath.
4	*	*		$-20 \pm 30$	185	1.0		$\text{Cu}_2\text{O}$ crystals, tin coat underneath? No visible attack.
101				$-50 \pm 20$			12 au	Tiny red spots. Otherwise excellent condition.
103				$-30 \pm 10$				Excellent conditions.
104	*			$-300/-30$		+0.04		Almost unchanged.

TABLE II Solution:  $\text{NaClO}_4 \cdot \text{N}_2$  Atmosphere

N	CPE	a.c.	Agar	d.c. V, mV	a.c. R, $\Omega \cdot \text{cm}^2$	s.c. c.d., $\mu\text{A}/\text{cm}^2$	Photo #	Visual Observation
3		*		-40±20	67			Almost black. Some indication of attack on extrusion lines, no pits. Perhaps some tin coat lift.
4	*	*		-40±10	186	+1.5		Dark green with protrusions. Extensive attack underneath. Small, shallow pits uniformly distributed.
101				-200/+10				Excellent conditions. Thin white patina.
103				+10±10				Almost unchanged.
112	*			+20±20		+0.14		Most tin coat can be removed by brushing. Otherwise little attack.

TABLE III Solution:  $\text{Na}_2\text{SO}_4 + \text{NaCl} \cdot \text{N}_2$  Atmosphere

N	CPE	a.c.	Agar	d.c. V, mV	a.c. R, $\Omega \cdot \text{cm}^2$	s.c. c.d., $\mu\text{A}/\text{cm}^2$	Photo #	Visual Observation
1	*	*		$-220 \pm 40$	16		11a	Uniform $\text{Cu}_2\text{O}$ layer, pits underneath, but also some tin coat left, some attack under the coat.
2	*	*		$-220 \pm 40$	30		13a	Similar to 1.
5	*	*		$-130 \pm 20$	14	+3.2		$\text{Cu}_2\text{O}$ , Cu deposit. Some small pits.
102				$-220 \pm 10$			12a1	Very little attack.
104				$-220 \pm 10$				Little attack. Maybe some loss of tin coat.
111	*			$-150 \pm 10$		+1.4		Light green patina. Part of the tin coat can be removed by scratching. Underneath is $\text{Cu}_2\text{O}$ , and probably pit initiation.
113	*			$-170 \pm 10$		+1.4		Similar to 111, but little can be removed by scratching.

TABLE IV Solution:  $\text{NaClO}_4 + \text{NaCl} \cdot \text{N}_2$  Atmosphere

N	CPE	a.c.	Agar	d.c. V, mV	a.c. R, $\Omega \cdot \text{cm}^2$	s.c. c.d., $\mu\text{A}/\text{cm}^2$	Photo #	Visual Observation
1		*		$-230 \pm 10$	40			$\text{Cu}_2\text{O}$ layer. Some pits underneath.
2		*		$-190 \pm 10$	30			Some fairly deep pits under the $\text{Cu}_2\text{O}$ layer.
5	*	*		$-100 \pm 10$	14	+3.2	14ab	Brushing removes salt scale and tin coat, showing grooved and attacked Cu wire.
102				$-170/-120$				Some tin coat can be removed by scratching. No pits.
104				$-100 \pm 20$				Most tin coat can be removed by scratching, but no pits.
111	*			$-120 \pm 20$		+1.4	13e	Tin coat can be brushed away easily.
113	*			$-120 \pm 20$		+1.4	13f	The tin coat crumbles away revealing attack underneath.

TABLE V Solution:  $\text{Na}_2\text{SO}_4$  - Oxygen Atmosphere

N	CPE	a.c.	Agar	d.c. V, mV	a.c. R, $\Omega \cdot \text{cm}^2$	s.c. c.d., $\mu\text{A}/\text{cm}^2$	Photo #	Visual Observation
7	*	*		$+30 \pm 10$	590	$+1/0.2$		Thin layer of green crystals. Some small pits. Large part of tin coat still in good condition.
8		*	*	$+5 \pm 20$	330		11b	Green scale. Red blisters. Some pitting under the scale.
10		*		$+20 \pm 10$	240		11d	Sheets and mounds of green salt. Extensive pitting with $\text{Cu}_2\text{O}$ in pits.
11		*		$+20 \pm 10$	250		11c	Same as 10.
106				$0 \pm 5$				Good condition.
107				$0 \pm 5$				Good condition.
109			*	$+35 \pm 5$				A few pits (2 or 3) under green mounds. Otherwise good.
115	*			$+10 \pm 5$		+0.14		Green crystals, white patina. Tinning in excellent condition.
117	*			$+15 \pm 5$		+0.2	13d	Green crystals. Tinning excellent.
118	*		*	$+18 \pm 5$		-0.14		White-green patina. - Excellent.

TABLE VI Solution: NaClO<sub>4</sub> • Oxygen Atmosphere

N	CPE	a.c.	Agar	d.c. V, mV	a.c. R, $\Omega \cdot \text{cm}^2$	s.c. c.d., $\mu\text{A}/\text{cm}^2$	Photo #	Visual Observation
7	*	*		+85±10	180	2.3		Green and black scale. Attack is not localized. Copper exposed in large areas, but some tinning still present.
8		*	*	+40±20	420		14cd	Only one pit, with Cu <sub>2</sub> O inside. Fairly extensive attack, but some tinning still on.
10		*		+55±15	260		15ab	Green-black scale. Pits under blisters.
11		*		+55±20	200			Same as 10. Tinning is intact on large areas.
106				+55±10				White-green patina in places. Excellent condition.
107				+55±10				More stains and black blisters than 106, but little attack underneath.
109			*	+70±10				Green patina in places. Tin coat can be removed by scratching, showing Cu <sub>2</sub> O formation, in one spot.
115				+65±10		0.35		Tin coat in good condition. Most red spots can be removed by scratching. Cu deposit?
117			*	+70±15		0.22		Tin coat in excellent condition.
118	*		*	+70±10		0.35		Good condition. Some loss of tin coat.

TABLE VII Solution:  $\text{Na}_2\text{SO}_4 + \text{NaCl} - \text{O}_2$  Atmosphere

N	CPE	a.c.	Agar	d.c. V, mV	a.c. R, $\Omega \cdot \text{cm}^2$	s.c. c.d., $\mu\text{A}/\text{cm}^2$	Photo #	Visual Observation
6	*	*		$-55 \pm 5$	420	-0.18	13b	Only one pit, distributed attack, considerable tin coat left. Small green crystals.
9		*	*	-150/-60	173			Green scale. Red blisters. Large and deep pits under salt mounds, but only at one level. Diff. aeration?
12		*		-40 up slowly	390		13c	Large green mounds. Pits under salt mounds not very deep. Probably no tinning left. Similar to NaClO <sub>4</sub> 12.
105				+20 up slowly			12b	Some loss of tinning, but little attack on copper.
108		*	*	-150/+65 steady				Green layer. Part of tin coat can be removed by scratching, but no extensive attack of copper.
110				$-10 \pm 10$				Tin layer has been attacked considerably. Some Cu attack. No obvious pit initiation.
114				$+30 \pm 20$			12c	Little attack. One spot could be pit initiation.
116	*			$-10 \pm 10$		-0.14		Some attack of tin coat. Otherwise excellent.
119	*		*	$-90 \pm 5$		+6.4	12d	Brittle surface layer than can be broken off easily. Red crystals underneath, but no pits.

TABLE VIII Solution:  $\text{NaClO}_4 + \text{NaCl} - \text{O}_2$  Atmosphere

N	CPE	a.c.	Agar	d.c. V, mV	a.c. R, $\Omega \cdot \text{cm}^2$	s.c. c.d., $\mu\text{A}/\text{cm}^2$	Photo #	Visual Observation
6	*	*		$0 \pm 10$	460	+0.2		Black-green layer with protrusions. Etching reveals some attack, but no pitting.
9		*	*	$-50 \pm 20$	120		14ef	Heavy attack at one level. Red and green crystals. Pits underneath. Good condition at top.
12		*		$-20$ $+60$ end	420		15cd	Green mounds, red inside. Pits.
105				$+10 \pm 10$				Some green salt. Good condition.
108			*	$-150$ $+70$				Top part good. Bottom part can be removed by scratching. $\text{Cu}_2\text{O}$ and attack under tin coat, but uniform. Pit initiation uncertain.
110				$+10 \pm 10$				Green layer. Tin coat can be removed by scratching, but little attack of copper.
116	*			$+50 \pm 10$		0.05	15e	Green salt and tin coat can be removed by scratching. No pits.
119	*		*	$-80 \pm 10$		+4.4	15f	Brittle layer. Copper corroded underneath.



## Figure Captions

1. Schematic circuit for corrosion tests with superimposed a.c.
2. Voltage signal (upper trace) and current signal (lower trace) for Cu in 2% Na<sub>2</sub>SO<sub>4</sub>.
3. Electrode potential vs. time for tinned Cu wire in 2% Na<sub>2</sub>SO<sub>4</sub>. N<sub>2</sub> atmosphere.
4. Electrode potential vs. time for tinned Cu wire in 2% Na<sub>2</sub>SO<sub>4</sub> + 1% NaCl. N<sub>2</sub> atmosphere.
5. Electrode potential vs. time for tinned Cu wire in 2% Na<sub>2</sub>SO<sub>4</sub>. O<sub>2</sub> atmosphere.
6. Electrode potential vs. time for tinned Cu wire in 2% Na<sub>2</sub>SO<sub>4</sub> + 1% NaCl. O<sub>2</sub> atmosphere.
7. Electrode potential vs. time for tinned Cu wire in 0.42 M NaClO<sub>4</sub>. N<sub>2</sub> atmosphere.
8. Electrode potential vs. time for tinned Cu wire in 0.42 M NaClO<sub>4</sub> + 1% NaCl. N<sub>2</sub> atmosphere.
9. Electrode potential vs. time for tinned Cu wire in 0.42 M NaClO<sub>4</sub>. O<sub>2</sub> atmosphere.
10. Electrode potential vs. time for tinned Cu wire in 0.42 M NaClO<sub>4</sub> + 1% NaCl. O<sub>2</sub> atmosphere.
11. Corrosion tests with superimposed a.c.
12. Corrosion tests without superimposed a.c.
13. Corrosion tests in Na<sub>2</sub>SO<sub>4</sub> and NaClO<sub>4</sub>.
14. Corrosion tests in NaClO<sub>4</sub>.
15. Corrosion tests in NaClO<sub>4</sub>.
16. Rest potentials vs. time of CPE and Pb-Sn alloy in 2% Na<sub>2</sub>SO<sub>4</sub> + 1% NaCl.
17. Potentiodynamic scans for tinned Cu in 2% Na<sub>2</sub>SO<sub>4</sub>. Scan rate 4 mV/sec. Dashed curve is expansion of solid curve and refers to c.d. scale on left.
18. Potentiodynamic scans for tinned Cu in 2% Na<sub>2</sub>SO<sub>4</sub> + 1% NaCl. Scan rate 4 mV/sec. Dashed curve is expansion of solid curve and refers to c.d. scale on left.
19. Potentiodynamic scans for Cu in 2% Na<sub>2</sub>SO<sub>4</sub>. Scan rate 4 mV/sec.
20. Potentiodynamic scans for Cu in 2% Na<sub>2</sub>SO<sub>4</sub> up to +800 mV. Scan rate 4 mV/sec.
21. Potentiodynamic scan for Cu in 0.42 M NaClO<sub>4</sub>. Inert atmosphere.

22. Potentiodynamic scans for Cu in 2% Na<sub>2</sub>SO<sub>4</sub> + 1% NaCl. Scan rate 4 mV/sec.
23. Potentiodynamic scans for Cu in 2% Na<sub>2</sub>SO<sub>4</sub> + 1% NaCl. Inert atmosphere.
24. Potentiodynamic scan for Cu in 2% Na<sub>2</sub>SO<sub>4</sub> + 1% NaCl. Inert atmosphere.
25. Potentiodynamic scans for Pb-Sn alloy in 2% Na<sub>2</sub>SO<sub>4</sub>. Scan rate 4 mV/sec.
26. Potentiodynamic scans for Pb-Sn alloy in 2% Na<sub>2</sub>SO<sub>4</sub> + 1% NaCl. Scan rate 4 mV/sec. Inert atmosphere.
27. Potentiodynamic scans for Pb-Sn alloy in 2% Na<sub>2</sub>SO<sub>4</sub> + 1% NaCl. Oxygen atmosphere. Scan rate 4 mV/sec.
28. Polarization curves for tinned Cu wire in 2% Na<sub>2</sub>SO<sub>4</sub>, taken in December 1976.
29. Polarization curves for tinned Cu wire in 2% Na<sub>2</sub>SO<sub>4</sub>, taken in January 1977.
30. X-ray spectra of various control specimens.
31. X-ray spectra of corroded neutral wires.
32. X-ray spectrum of corroded CCN wire #119. Solution 2% Na<sub>2</sub>SO<sub>4</sub> + 1% NaCl, O<sub>2</sub> atmosphere, CPE coupling, Agar, 1600 h.
33. Schematic circuit for noise measurements.
34. Noise spectrum at open circuit.
35. Noise spectra of Fe in 1:1 H<sub>3</sub>BO<sub>3</sub>-Na<sub>2</sub>B<sub>4</sub>O<sub>7</sub>+0.01 M NaCl at various potentials.
36. Oscillographic record of electrode potential of Fe in 1:1 H<sub>3</sub>BO<sub>3</sub>-Na<sub>2</sub>B<sub>4</sub>O<sub>7</sub>+0.01 M NaCl above and below the pitting potential.
37. Noise measuring circuit.
38. Spectral power amplitude vs. frequency. Noise generated by the instrumentation and by a 10 K $\Omega$  resistor.
39. a) Coated copper wire specimen.  
b) Bare copper wire specimen.
40. a) Conducting polyethylene specimen.  
b) Coating alloy sheet specimen.
41. Plan of NBS underground corrosion test site.

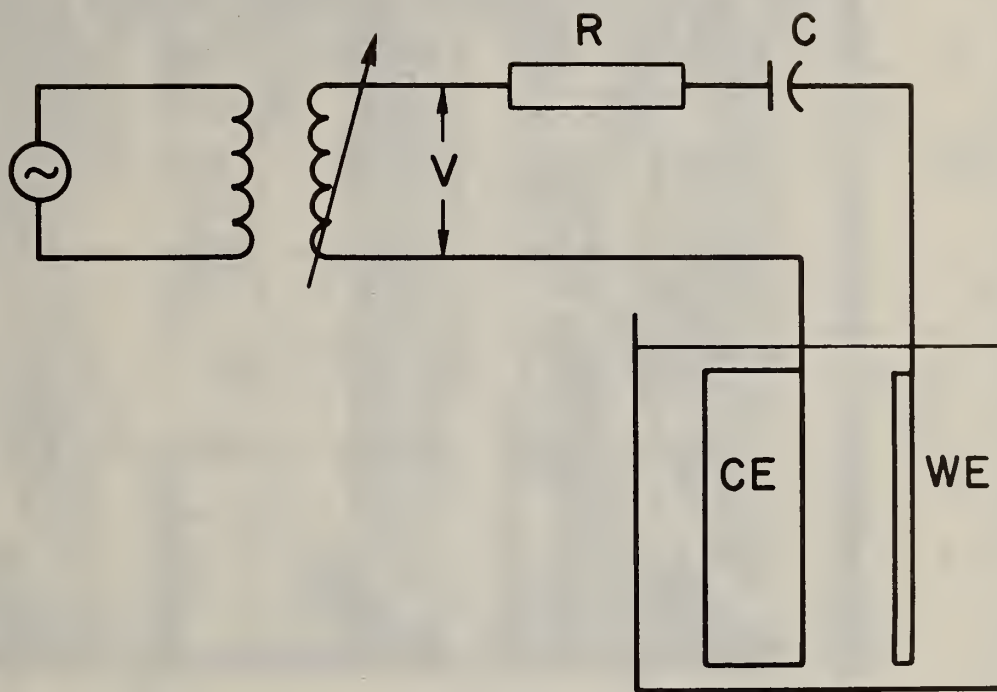
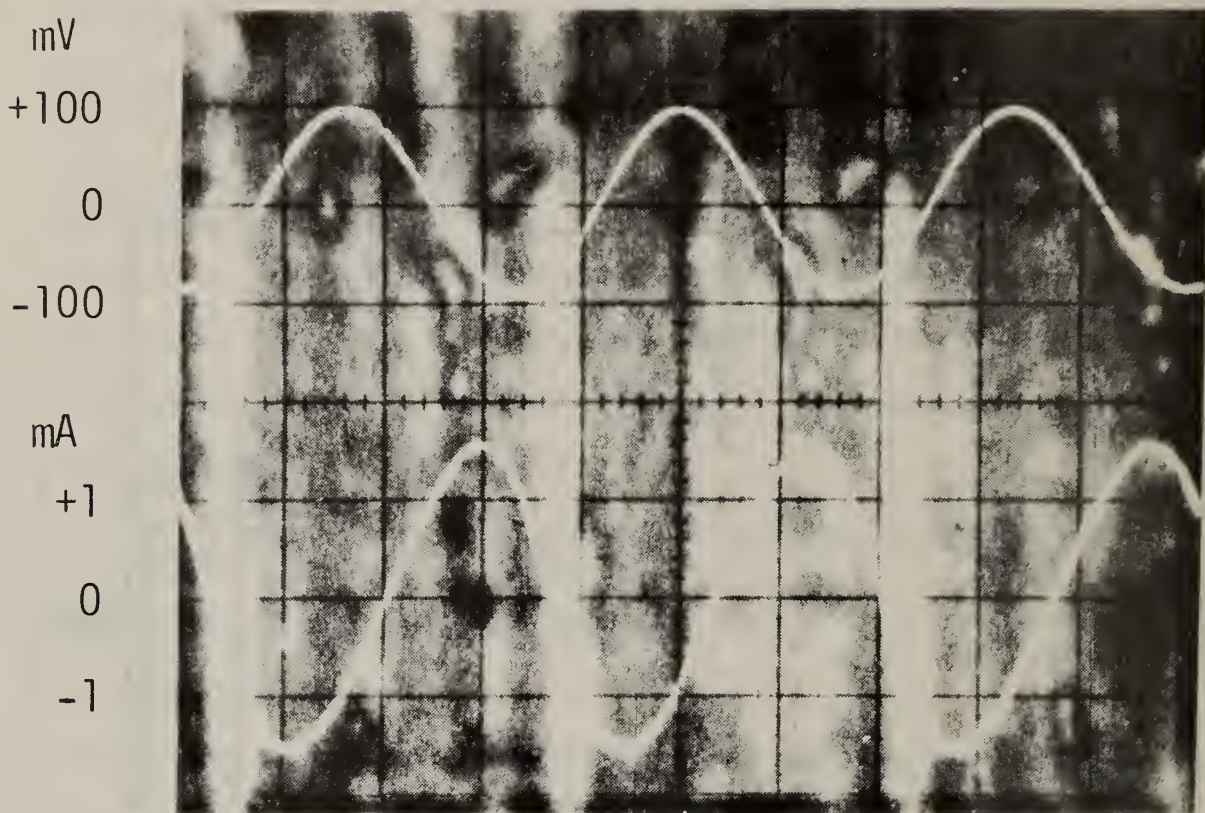


Fig. 1. Schematic circuit for corrosion tests with superimposed a.c.



Sweep rate 5 ms/div

Fig. 2. Voltage signal (upper trace) and current signal (lower trace) for Cu in 2%  $\text{Na}_2\text{SO}_4$ .

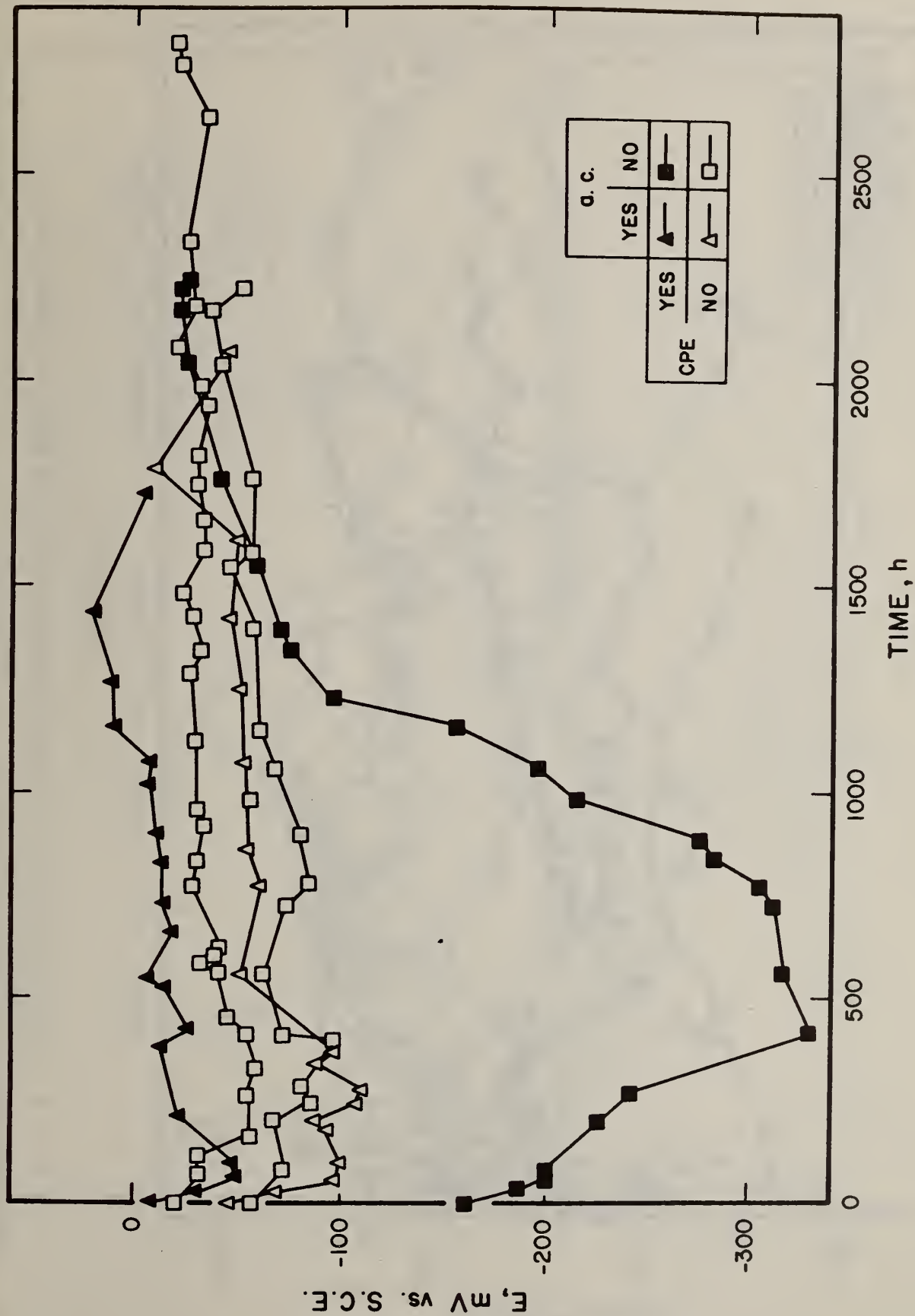


Fig. 3. Electrode potential vs. time for tinned Cu wire in 2%  $\text{Na}_2\text{SO}_4$ .  $\text{N}_2$  atmosphere.

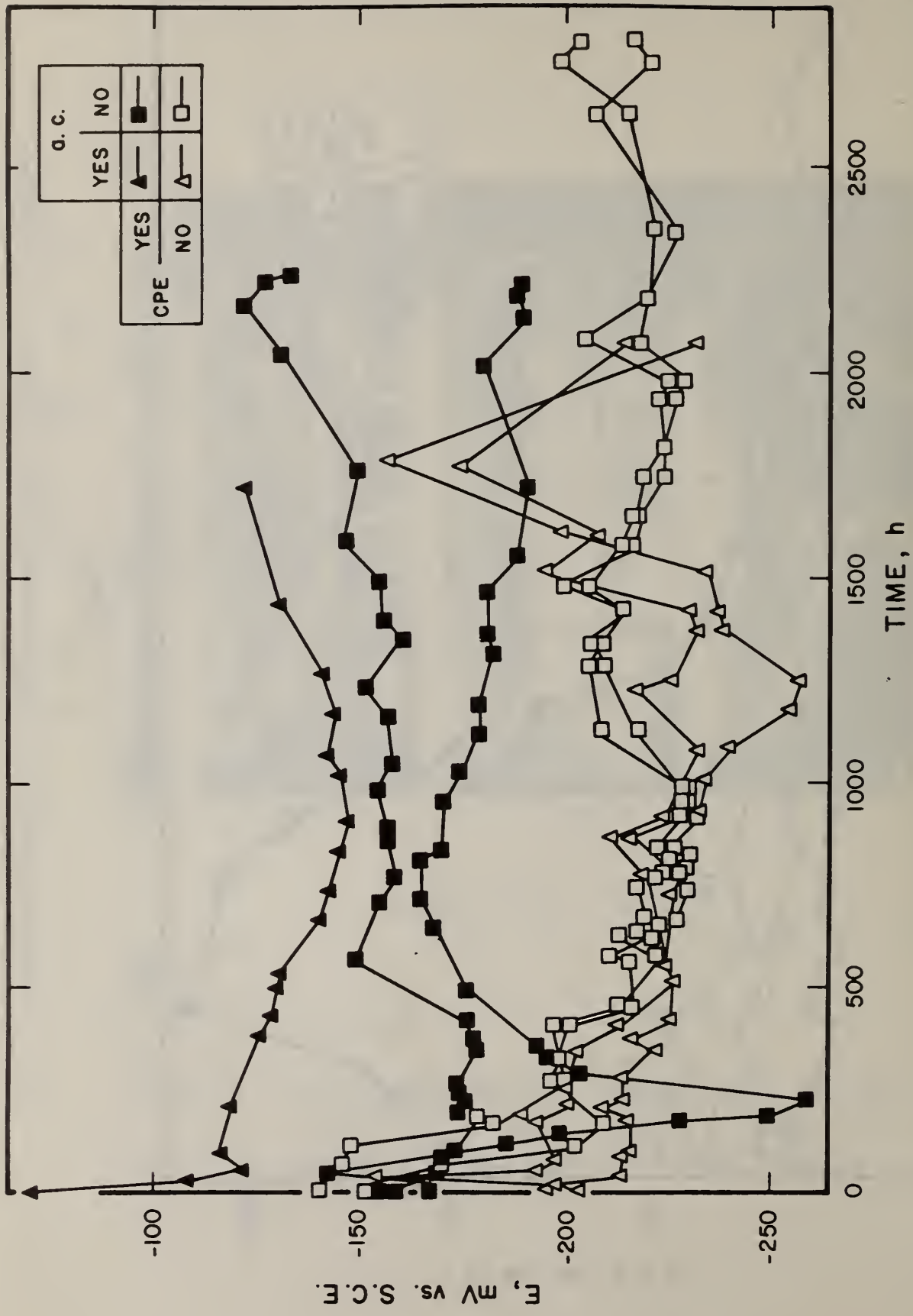


Fig. 4. Electrode potential vs. time for tinned Cu wire in 2% Na<sub>2</sub>SO<sub>4</sub> + 1% NaCl. N<sub>2</sub> atmosphere.

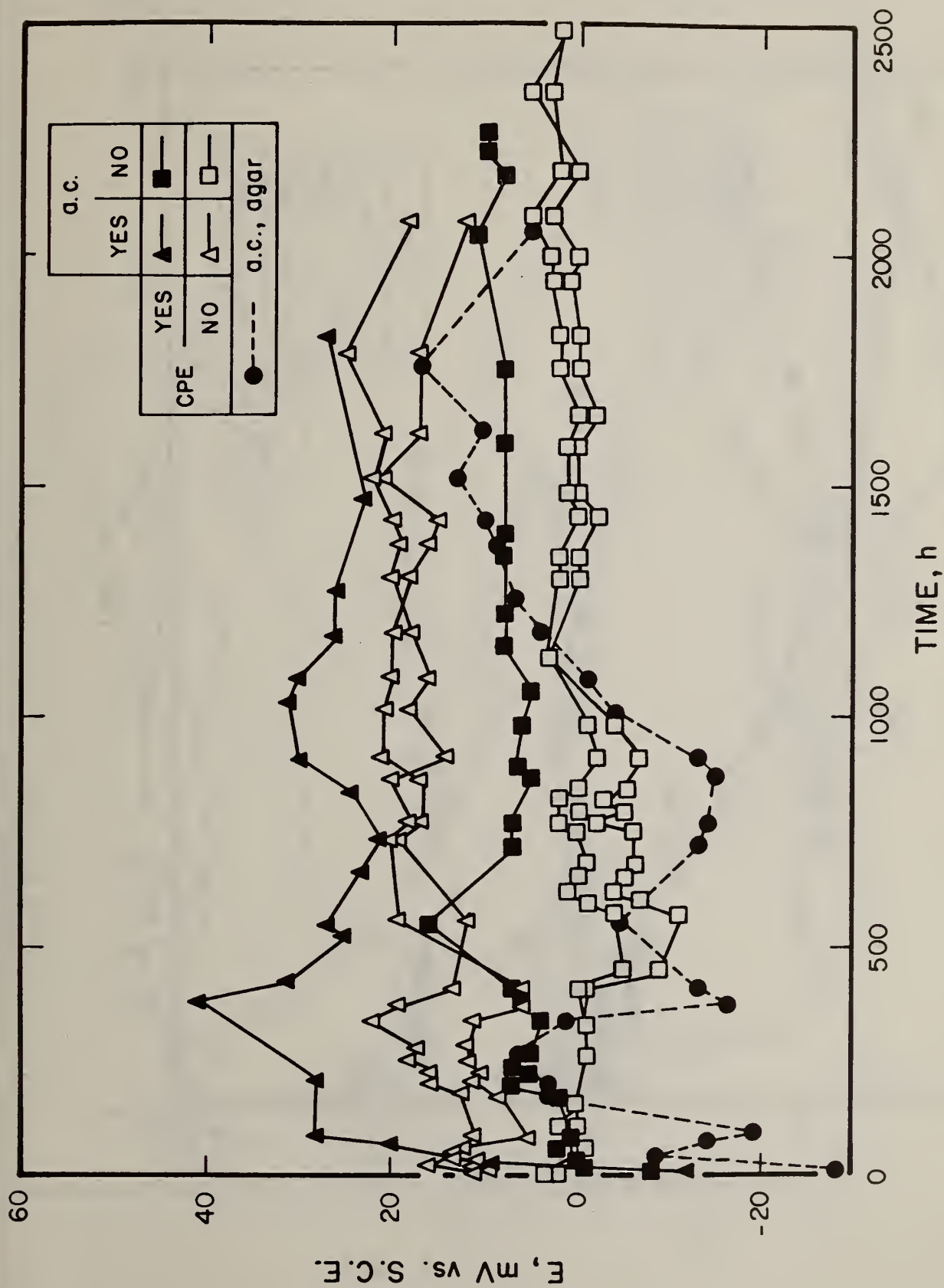


Fig. 5. Electrode potential vs. time for tinned Cu wire in 2%  $\text{Na}_2\text{SO}_4$ .  $\text{O}_2$  atmosphere.

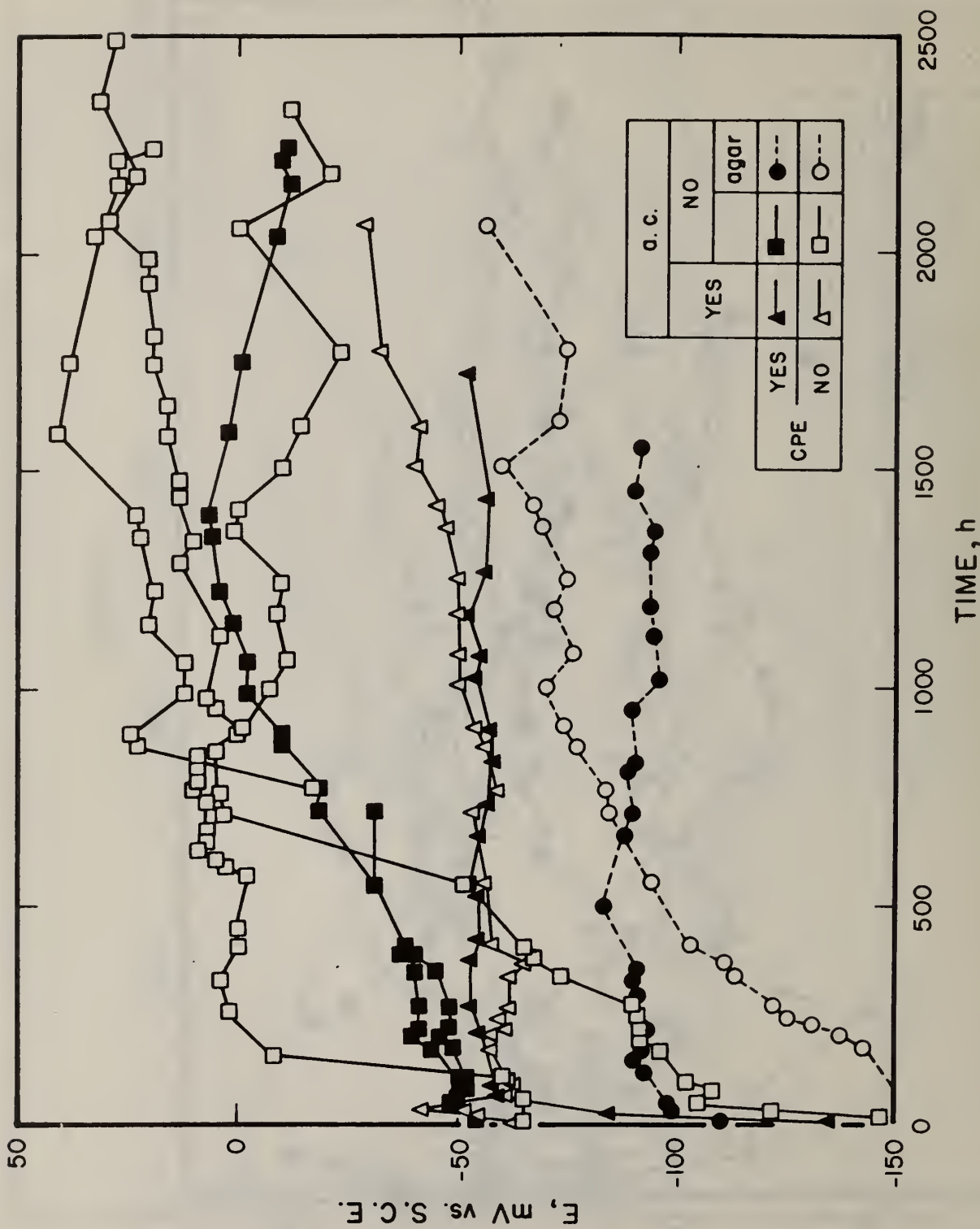


Fig. 6. Electrode potential vs. time for tinned Cu wire in 2% Na<sub>2</sub>SO<sub>4</sub> + 1% NaCl. O<sub>2</sub> atmosphere.

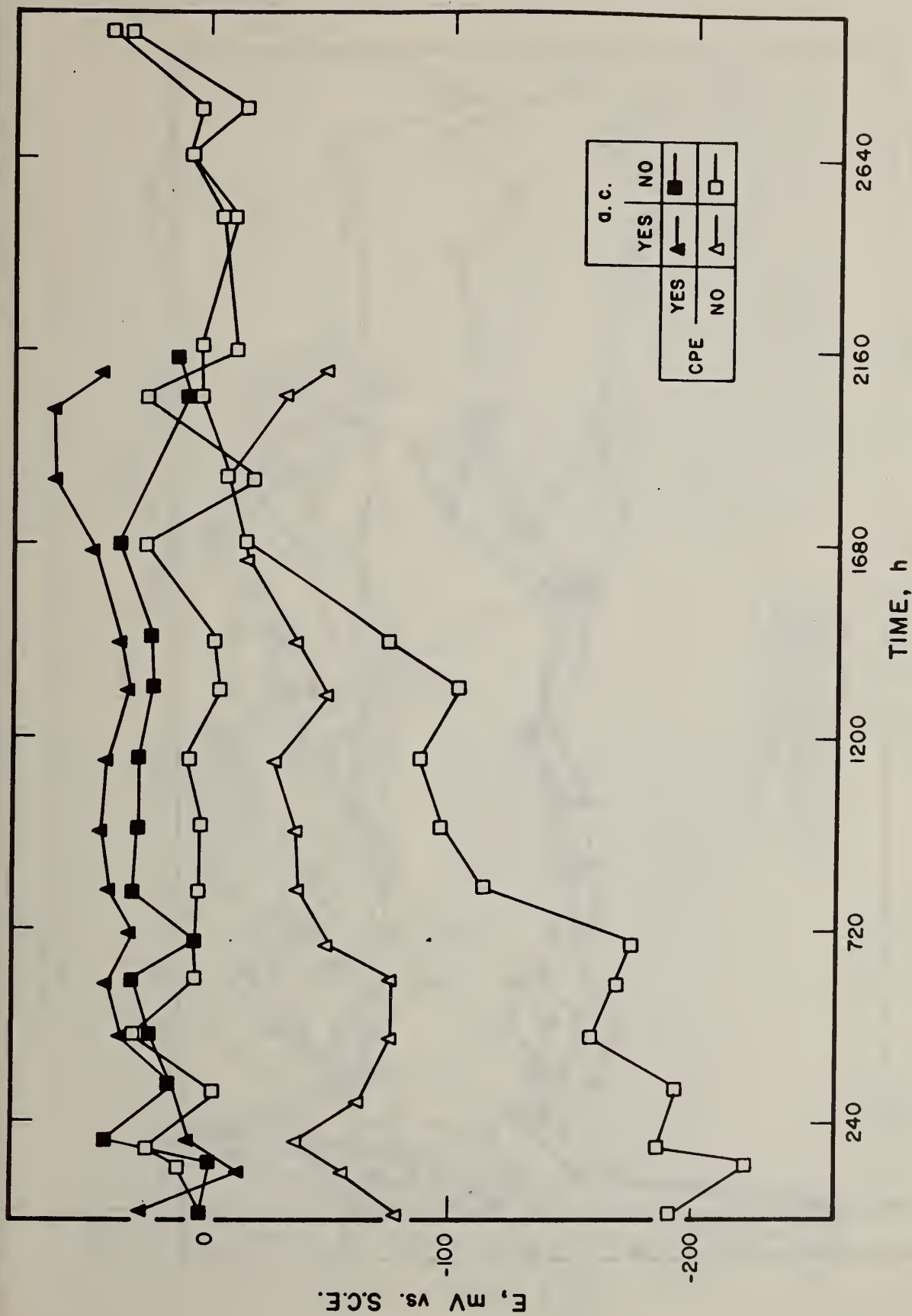


Fig. 7. Electrode potential vs. time for tinned Cu wire in 0.42 m NaClO<sub>4</sub>. N<sub>2</sub> atmosphere.

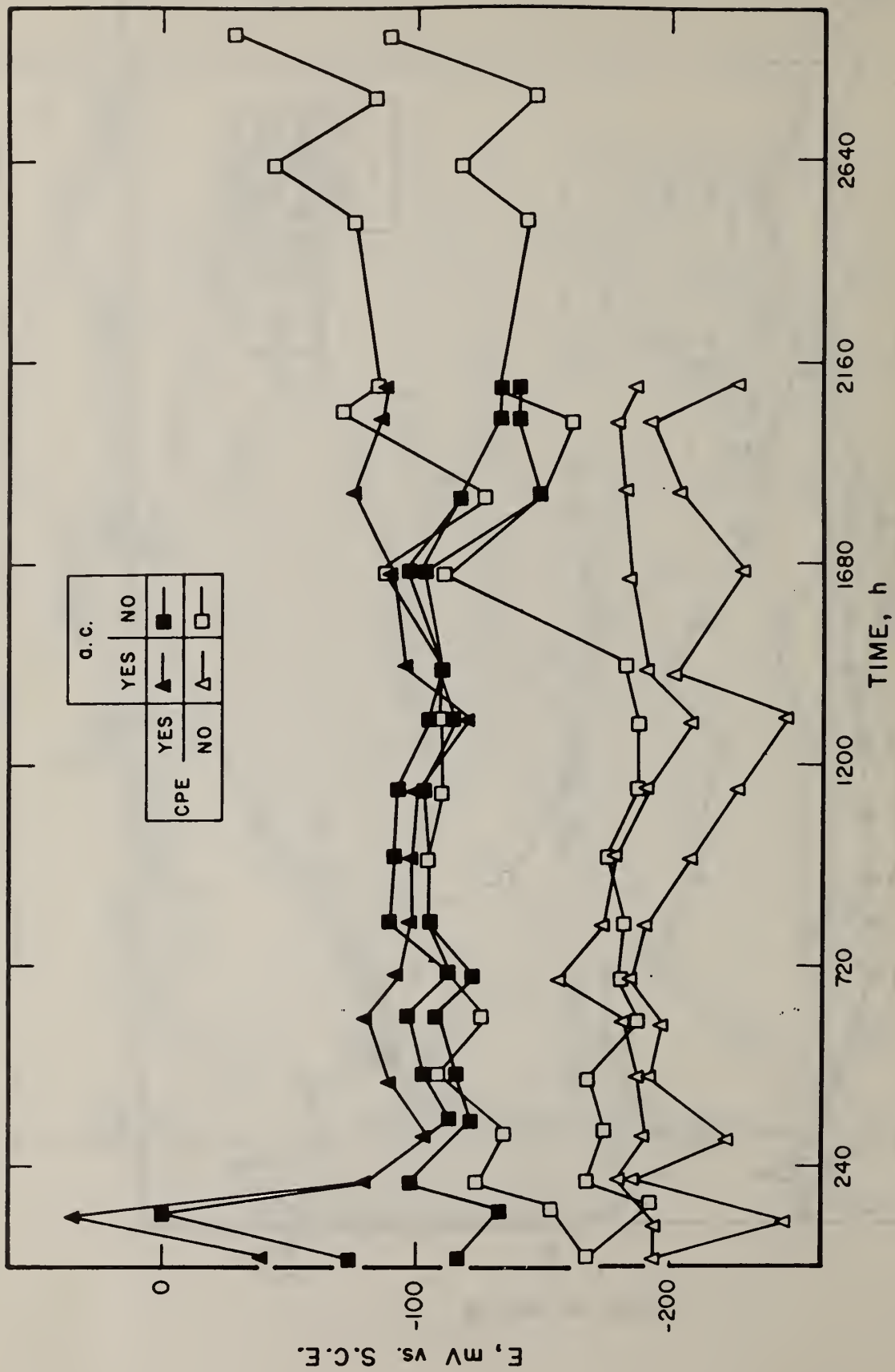


Fig. 8. Electrode potential vs. time for tinned Cu wire in 0.42 M NaClO<sub>4</sub> + 1% NaCl. N<sub>2</sub> atmosphere.

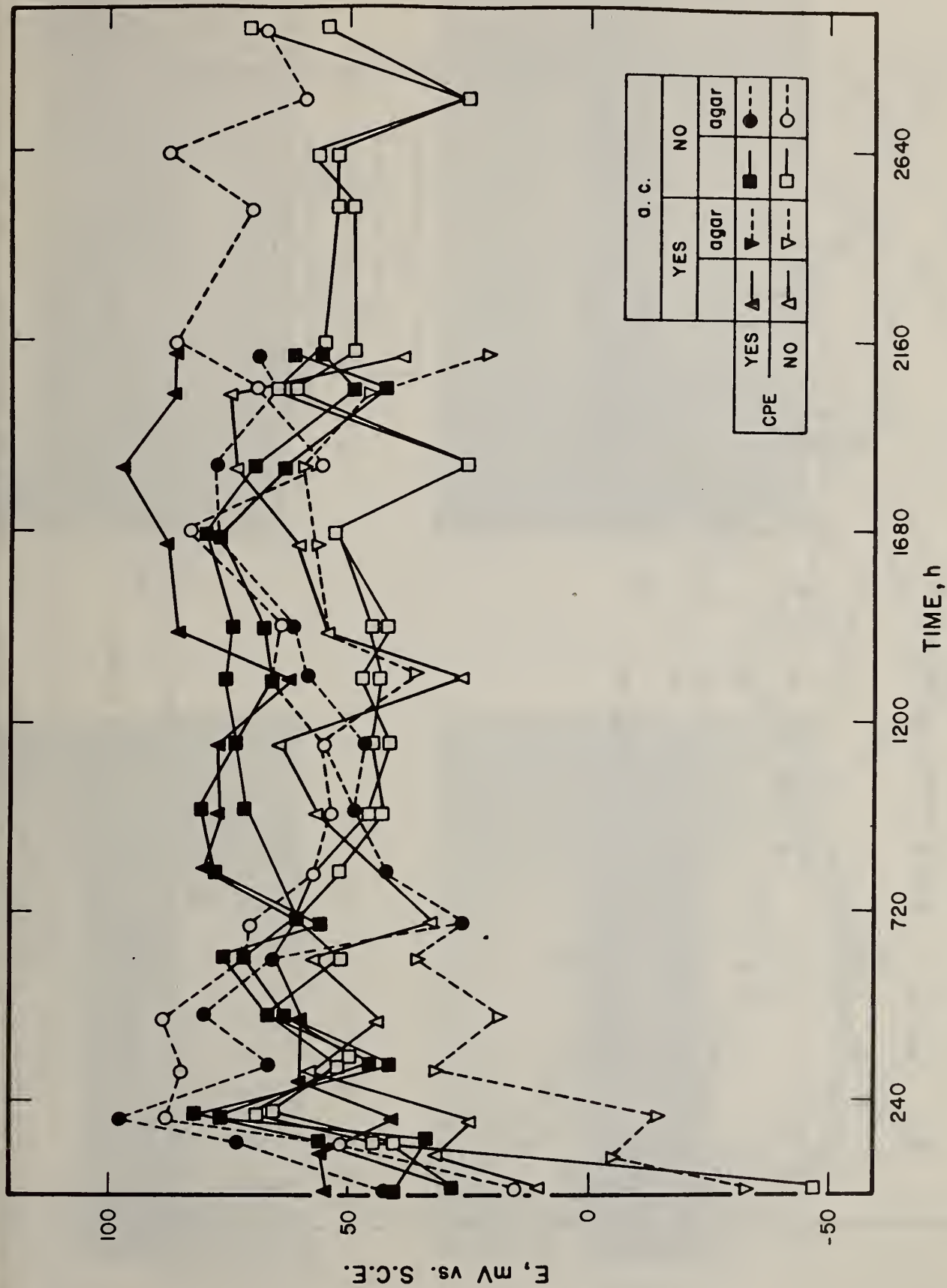


Fig. 9. Electrode potential vs. time for tinned Cu wire in 0.42 M NaClO<sub>4</sub>, 0<sub>2</sub> atmosphere.

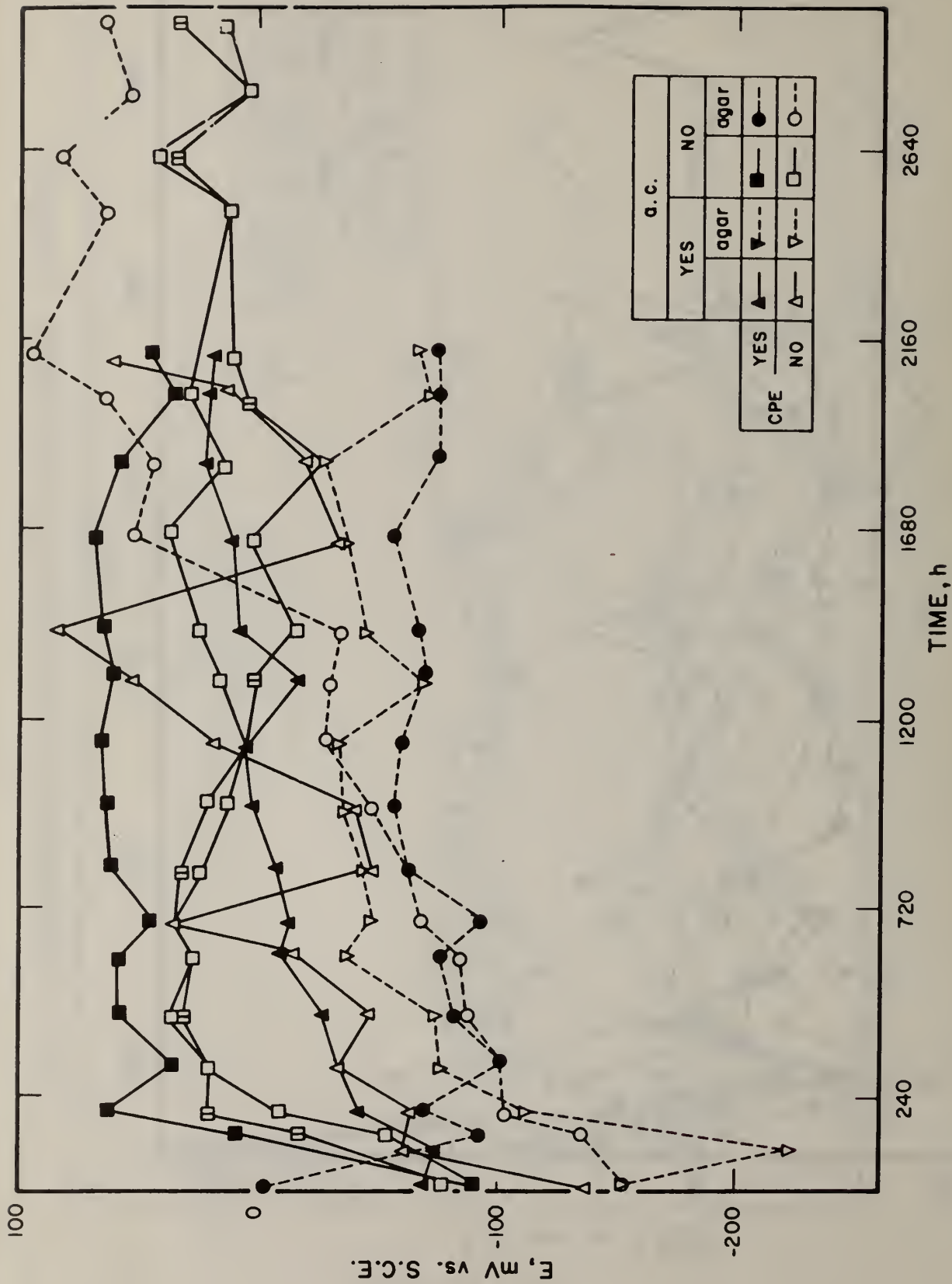
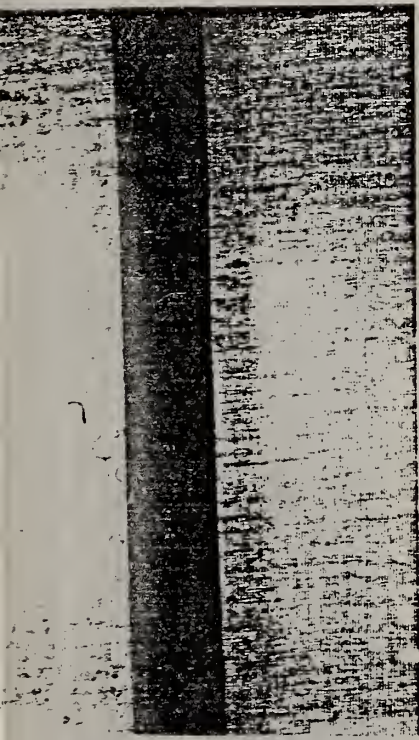
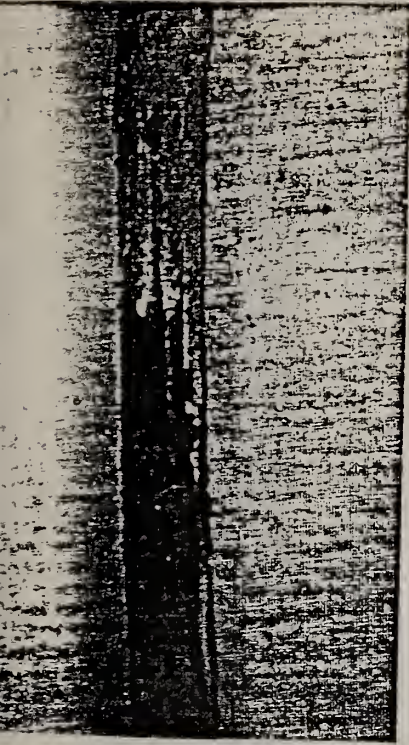


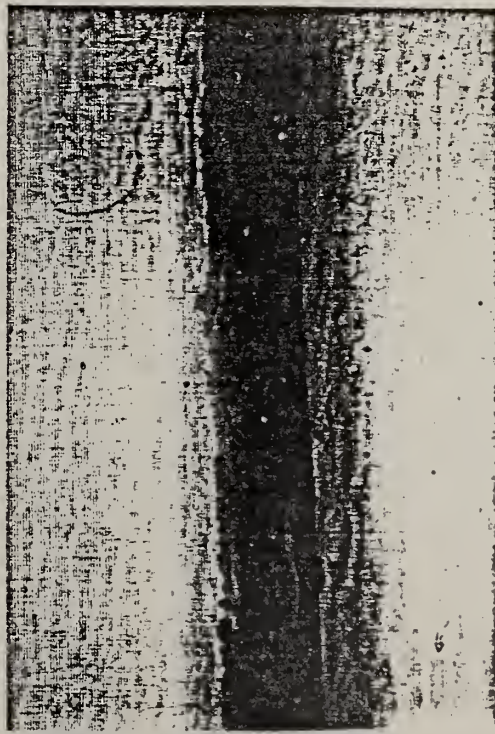
Fig. 10. Electrode potential vs. time for tinned Cu wire in 0.42 M NaClO<sub>4</sub> + 1% NaCl. O<sub>2</sub> atmosphere.



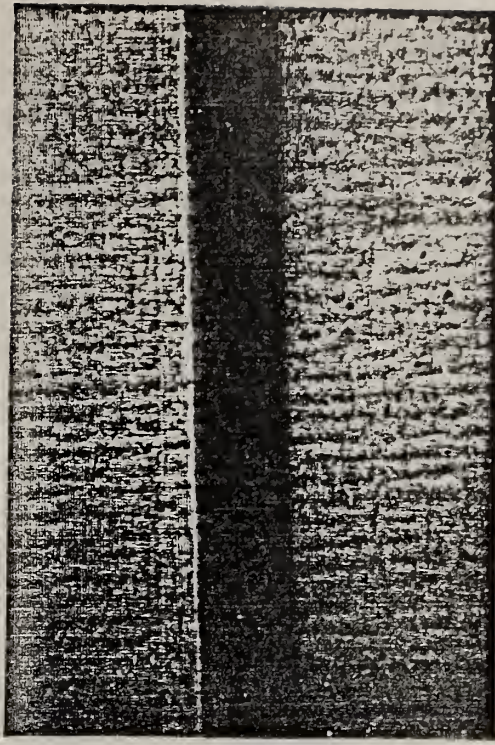
a) #1. N<sub>2</sub>. Chloride. 2000 h.



b) #8. O<sub>2</sub>. Sulfate. Agar. 2000 h.



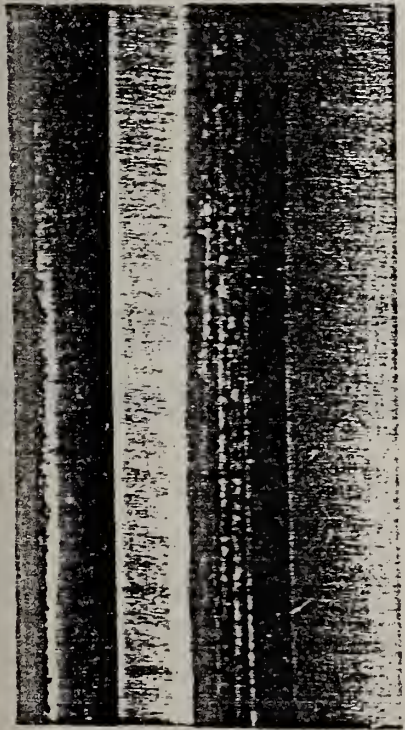
c) #11. O<sub>2</sub>. Sulfate. 2000 h.



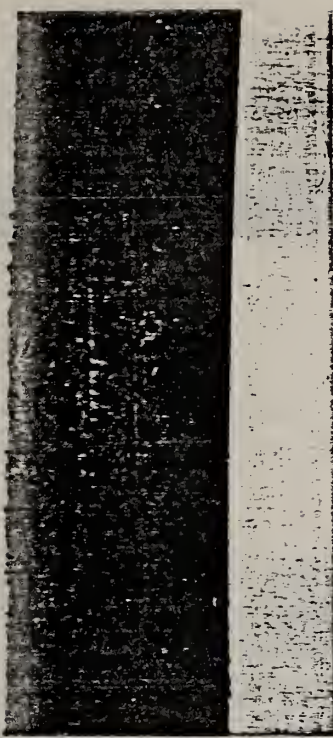
d) #10. O<sub>2</sub>. Sulfate. 2000 h.  
After removing salt scale.

Fig. 11. Corrosion tests with superimposed a.c.

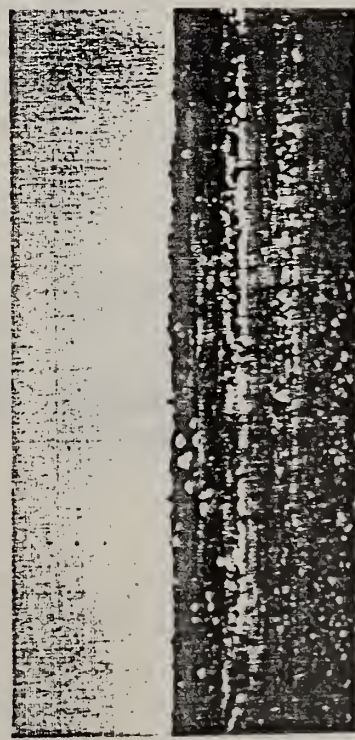




a) Upper #101.  $\text{H}_2\text{SO}_4$ . Sulfate. 2800 h.  
Lower #102.  $\text{H}_2\text{SO}_4$ . Chloride. 2800 h.



b) #105.  $\text{O}_2$ . Chloride. 2800 h.

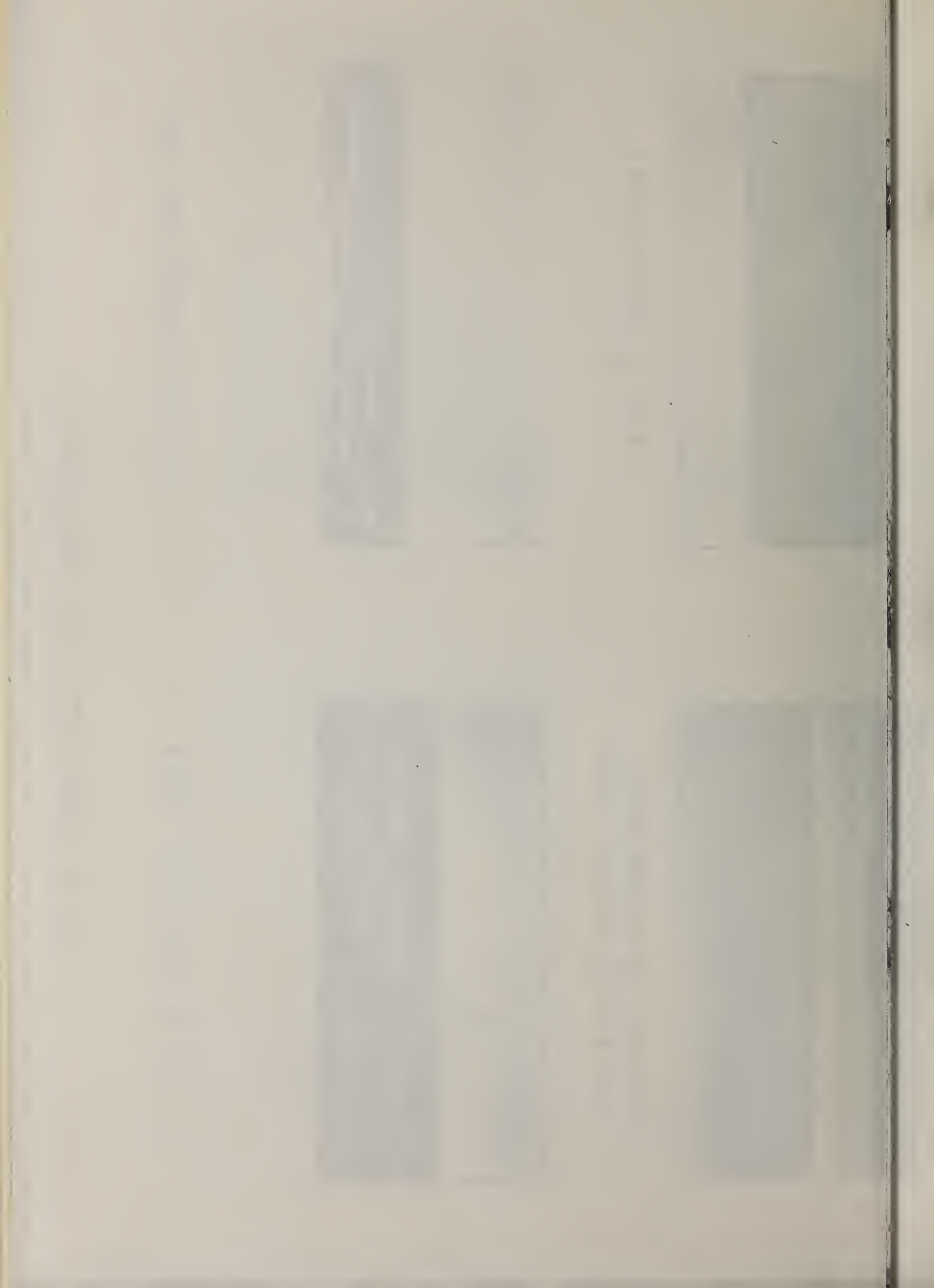


c) # 114.  $\text{O}_2$ . Chloride. CPE. 2200 h.



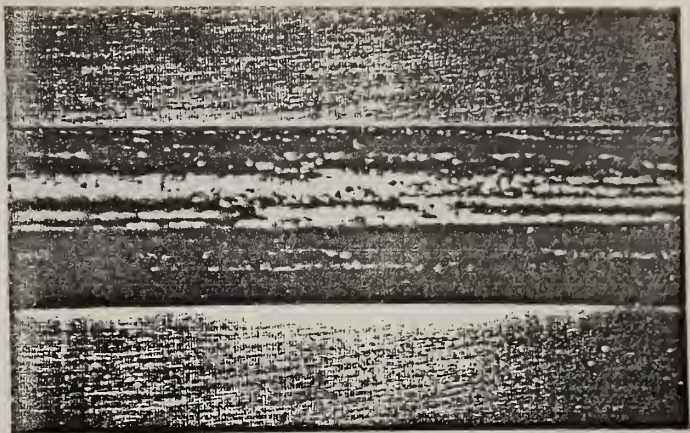
d) #119.  $\text{O}_2$ . Chloride. Agar. 2200 h.

Fig. 12. Corrosion tests without superimposed a.c.





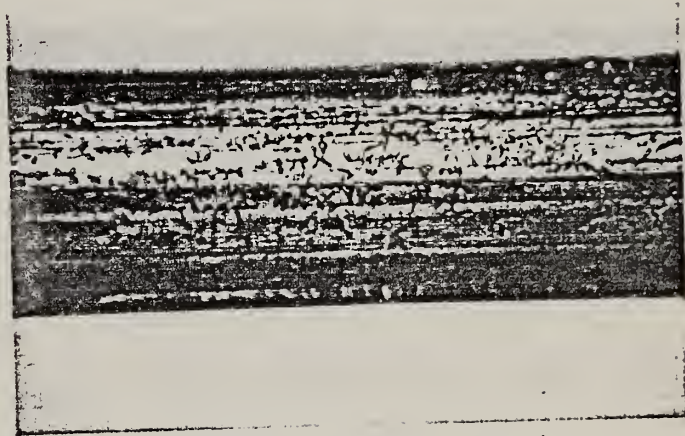
a) #2. Sulfate,  $N_2$ ,  $Cl^-$ , a.c. 2100 h  
After scratching and cleaning in acid.



b) #6. Sulfate,  $O_2$ , CPE,  $Cl^-$ , a.c. 1720 h  
After scratching and cleaning in acid.



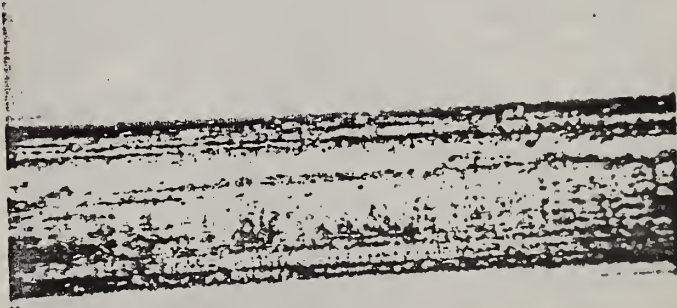
c) #12. Sulfate,  $O_2$ ,  $Cl^-$ , a.c. 2100 h  
After scratching and cleaning in acid.



d) #117. Sulfate,  $O_2$ , CPE, 2100 h



e) #111. Perchlorate,  $N_2$ ,  $Cl^-$ , CPE, 2100 h



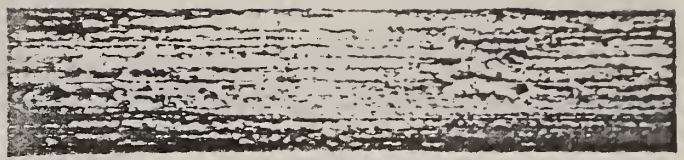
f) #113. Perchlorate,  $N_2$ ,  $Cl^-$ , CPE, 2100 h  
After brushing.

Fig. 13. Corrosion Tests in  $Na_2SO_4$  and  $NaClO_4$ .





a) #5.  $N_2$ , CPE,  $Cl^-$ , a.c. 2100 h



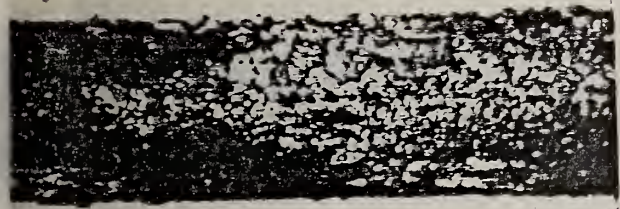
b) #5. After brushing.



c) #8.  $O_2$ , Agar, a.c. 2100 h



d) #8. After scratching and cleaning in acid.



e) #9.  $O_2$ ,  $Cl^-$ , a.c., Agar. 2100 h



f) #9. After scratching and cleaning in  $HNO_3$ .

Fig. 14. Corrosion Tests in  $NaClO_2$ .





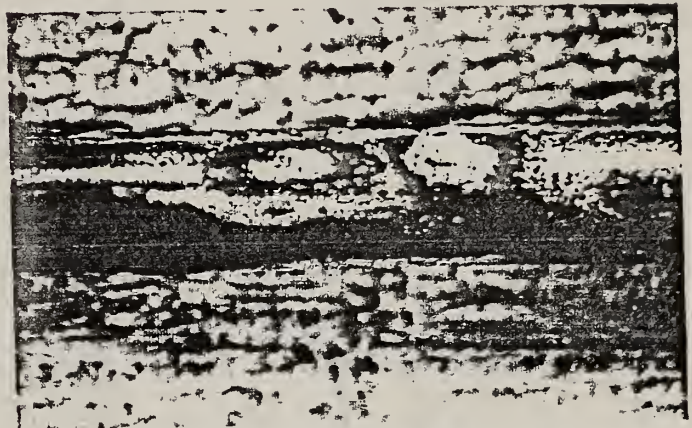
a) #10.  $O_2$ , a.c. 2100 h



b) #10. After scratching and cleaning in acid.



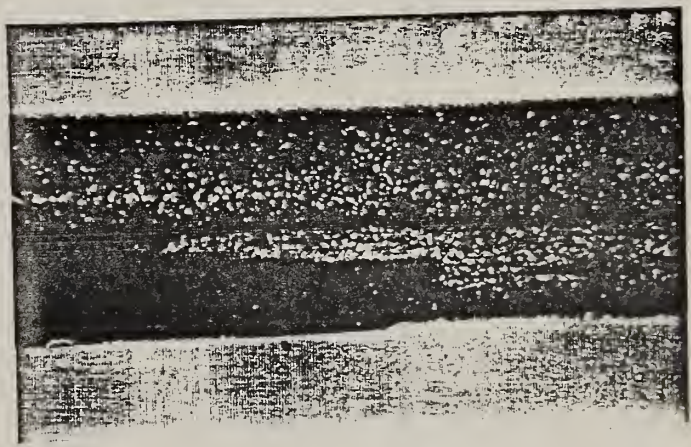
c) #12.  $O_2$ ,  $Cl^-$ , a.c. 2100 h



d) #12. After scratching and cleaning in acid.



e) #116.  $O_2$ , CPE,  $Cl^-$ , 2100 h



f) #119.  $O_2$ , CPE, Anar,  $Cl^-$ , 2200 h. Scale partially removed.

Fig. 15. Corrosion Tests in  $H_2ClO_4$ .



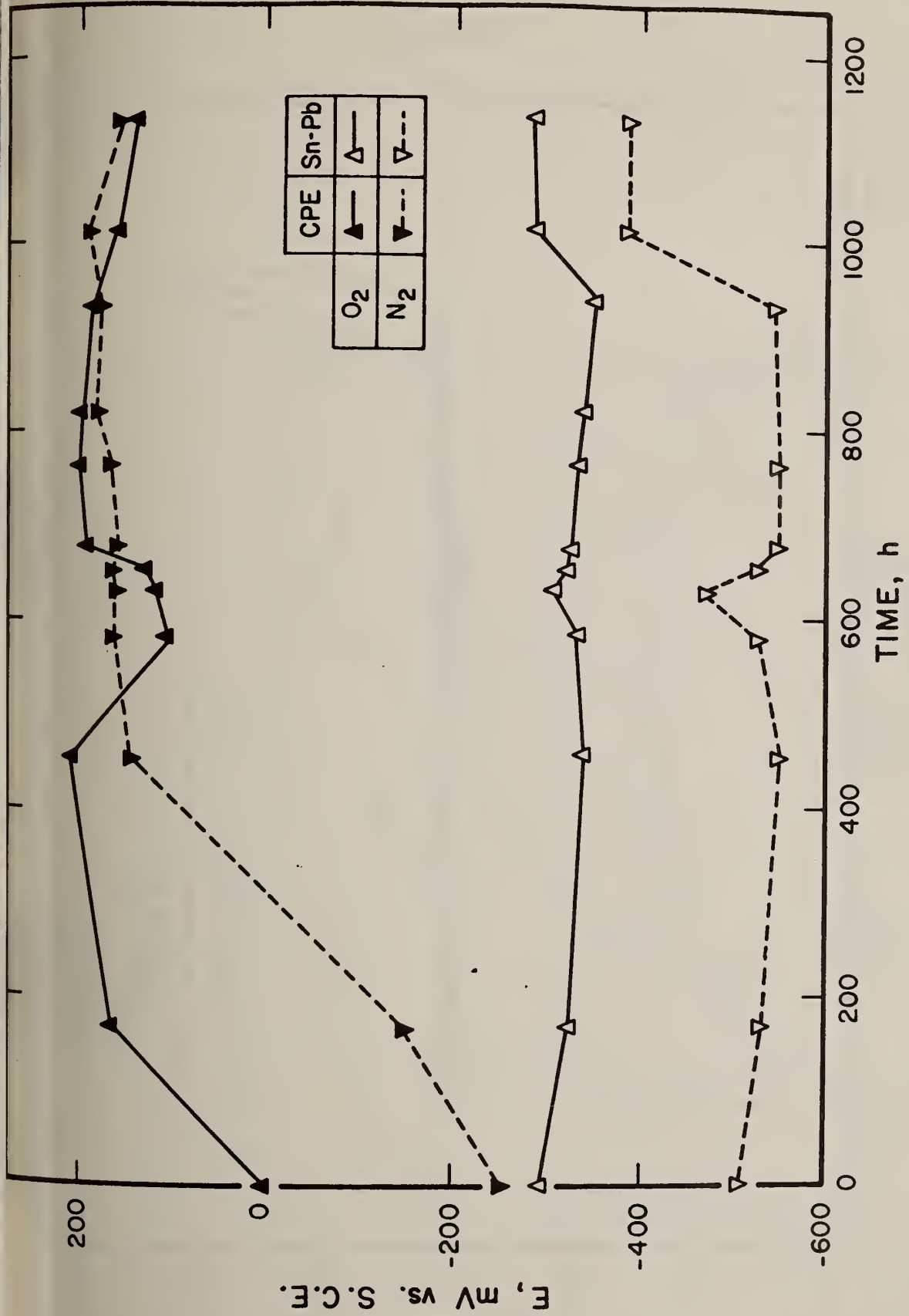


Fig. 16. Rest potentials vs. time of CPE and Pb-Sn alloy in 2% Na<sub>2</sub>SO<sub>4</sub> + 1% NaCl.



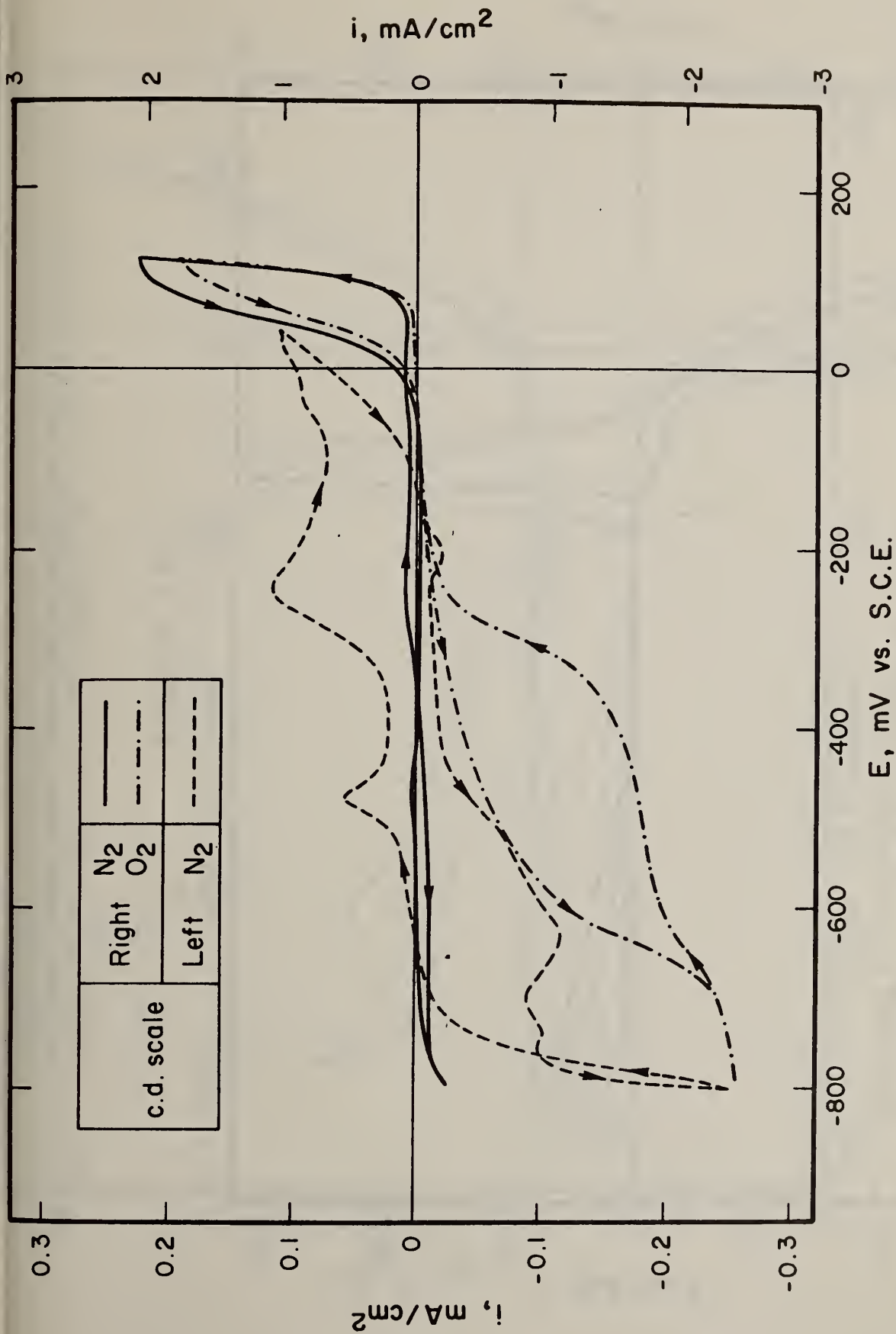


Fig. 17. Potentiodynamic scans for tinned Cu in 2% Na<sub>2</sub>SO<sub>4</sub>. Scan rate 4 mV/sec. Dashed curve is expansion of solid curve and refers to c.d. scale on left.

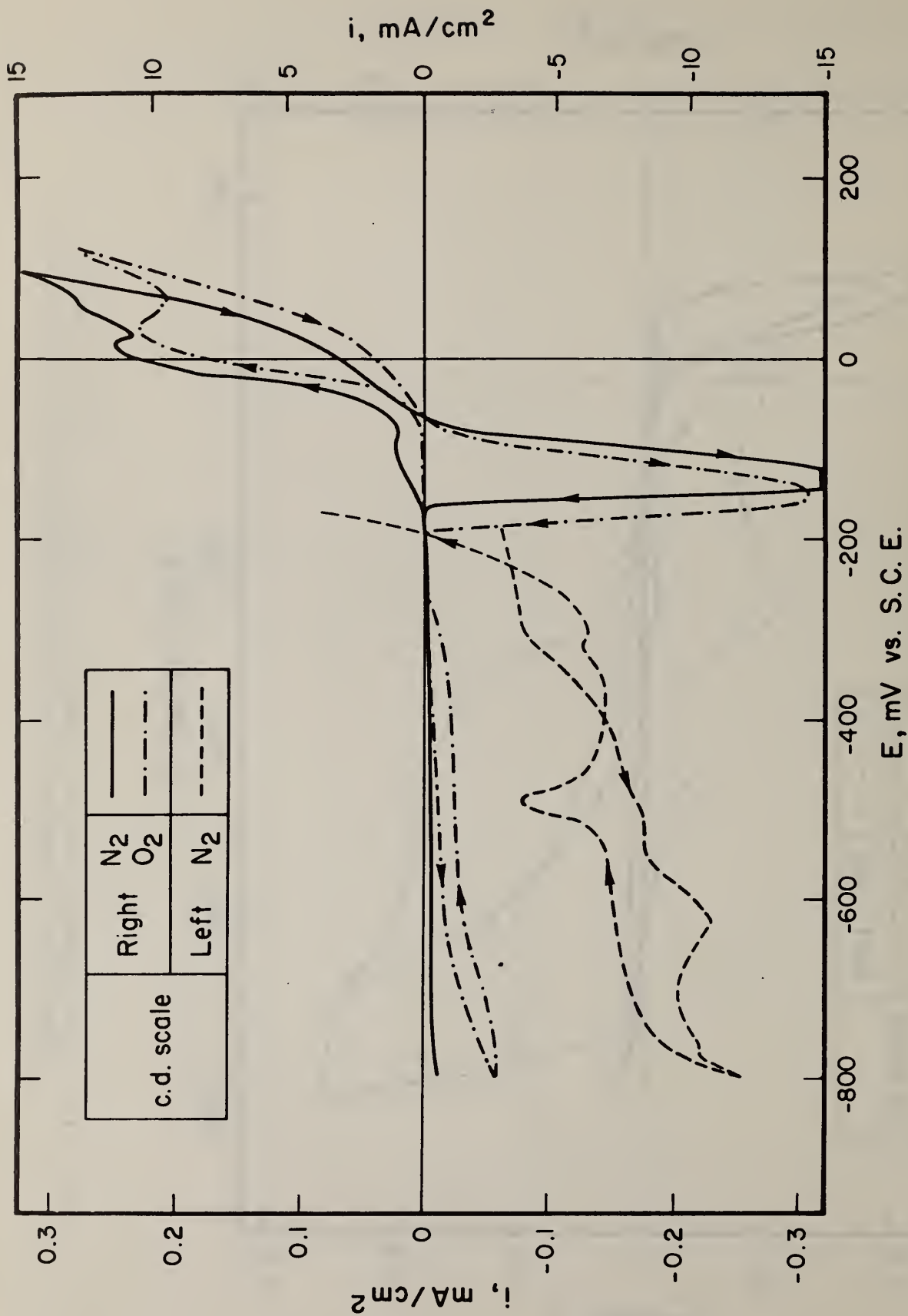


Fig. 18. Potentiodynamic scans for tinned Cu in 2% Na<sub>2</sub>SO<sub>4</sub> + 1% NaCl. Scan rate 4 mV/sec. Dashed curve is expansion of solid curve and refers to c.d. scale on left.

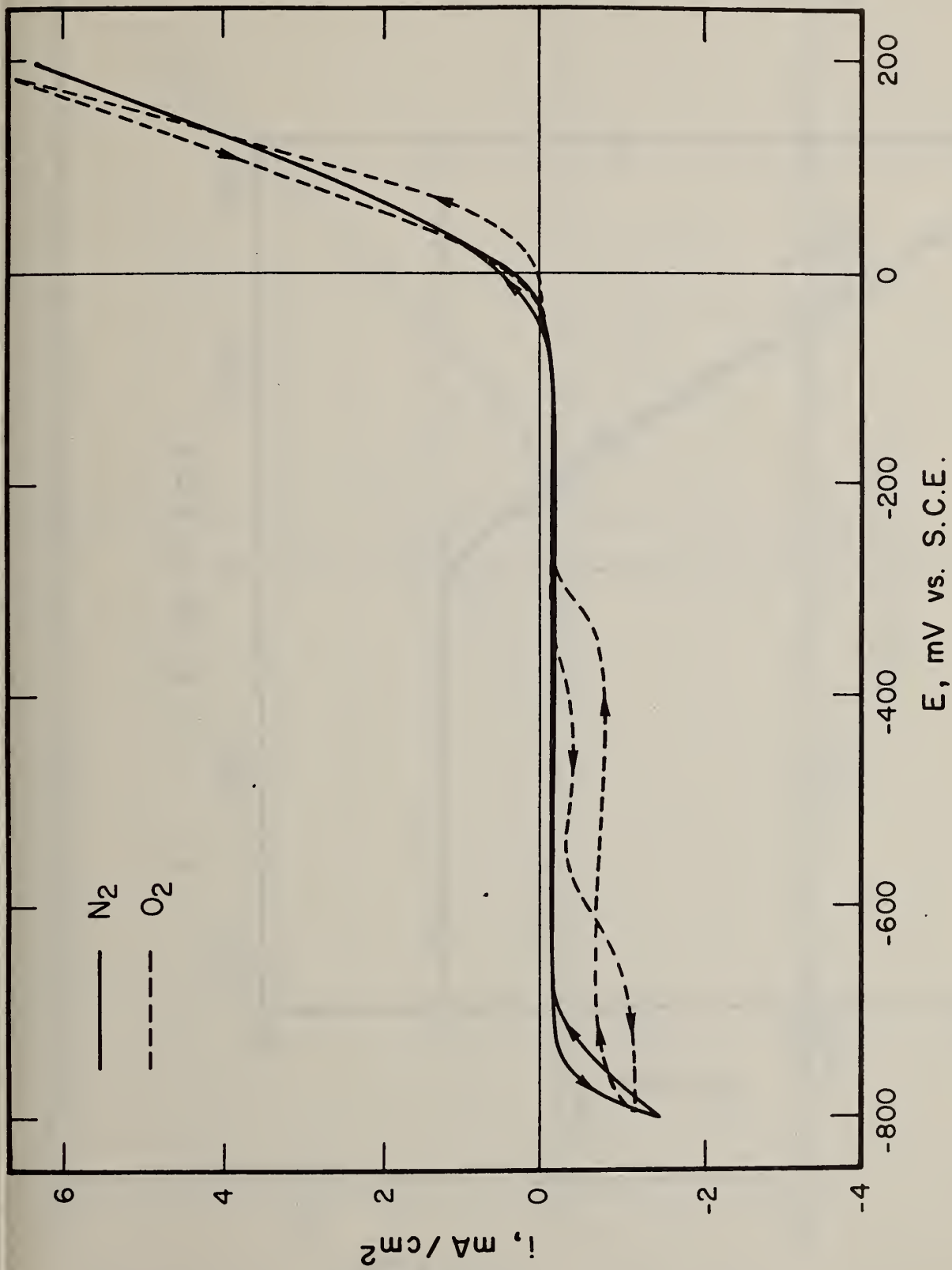


Fig. 19. Potentiodynamic scans for Cu in 2% Na<sub>2</sub>SO<sub>4</sub>. Scan rate 4 mV/sec.

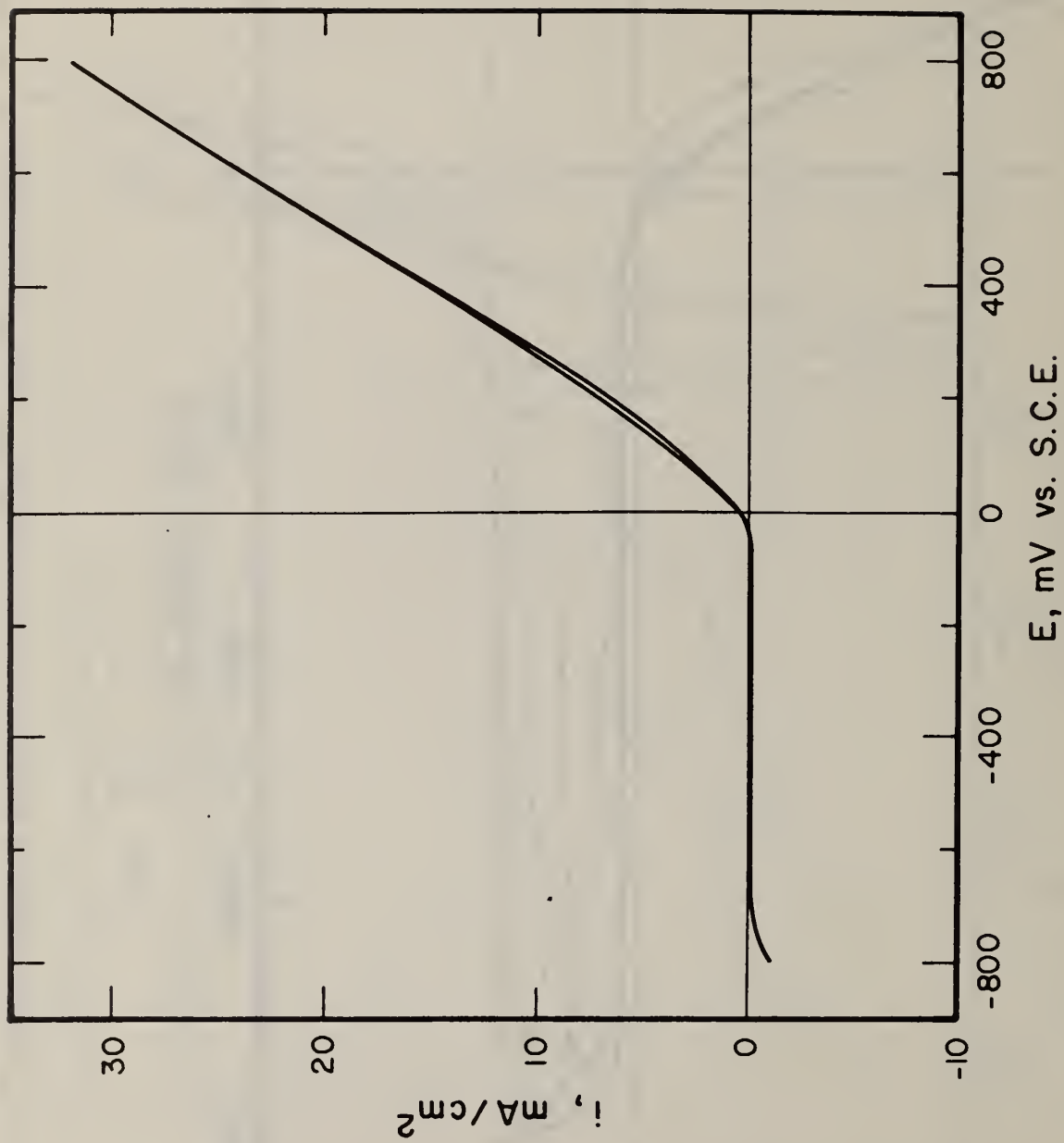


Fig. 20. Potentiodynamic scans for Cu in 2 M Na<sub>2</sub>SO<sub>4</sub> up to +800 mV. Scan rate 4 mV/sec.

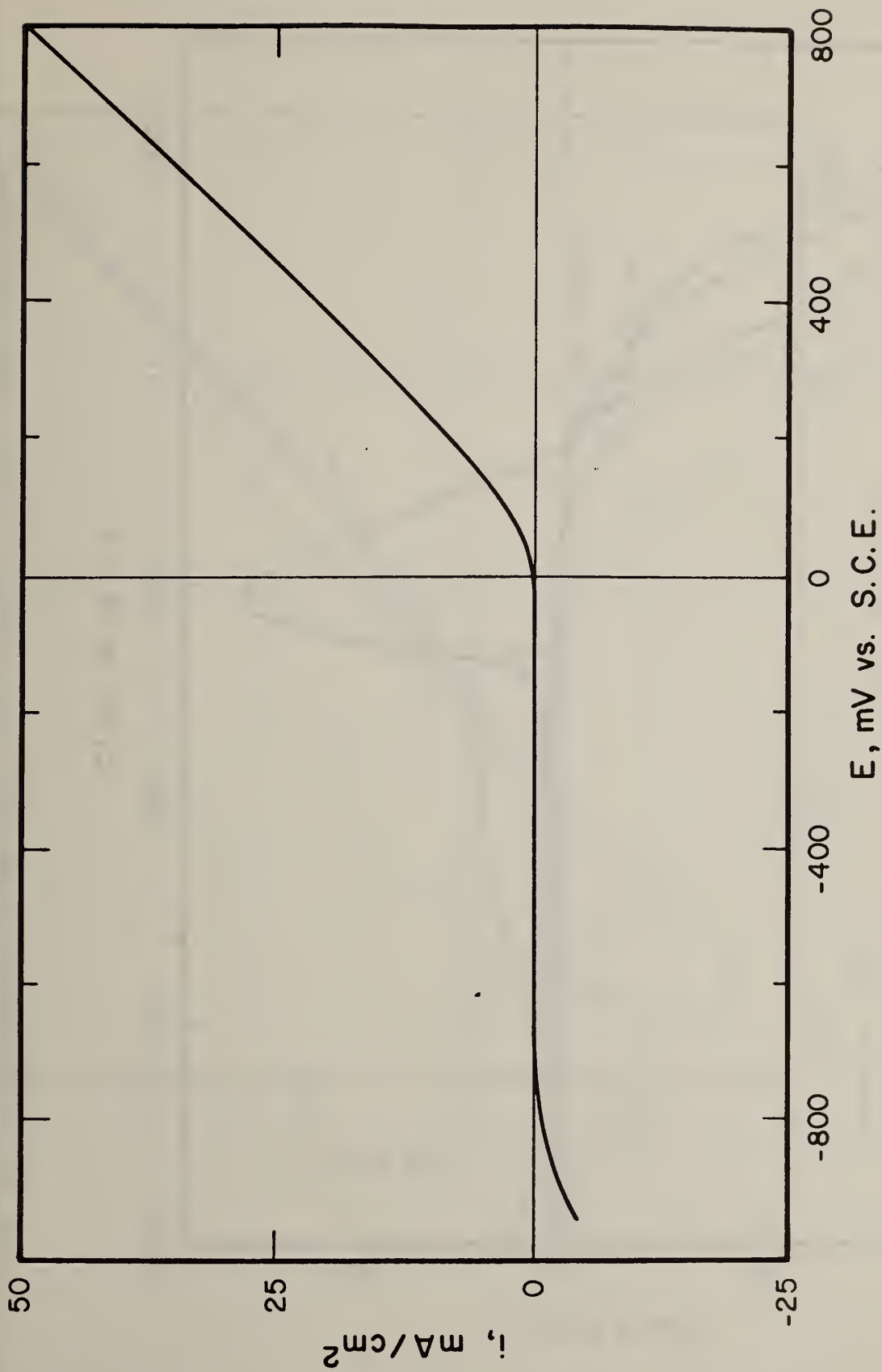


Fig. 21. Potentiodynamic scan for Cu in 0.42 M  $\text{NaClO}_4$ . Inert atmosphere.  
Scan rate 4  $\text{mV}/\text{sec}$ .

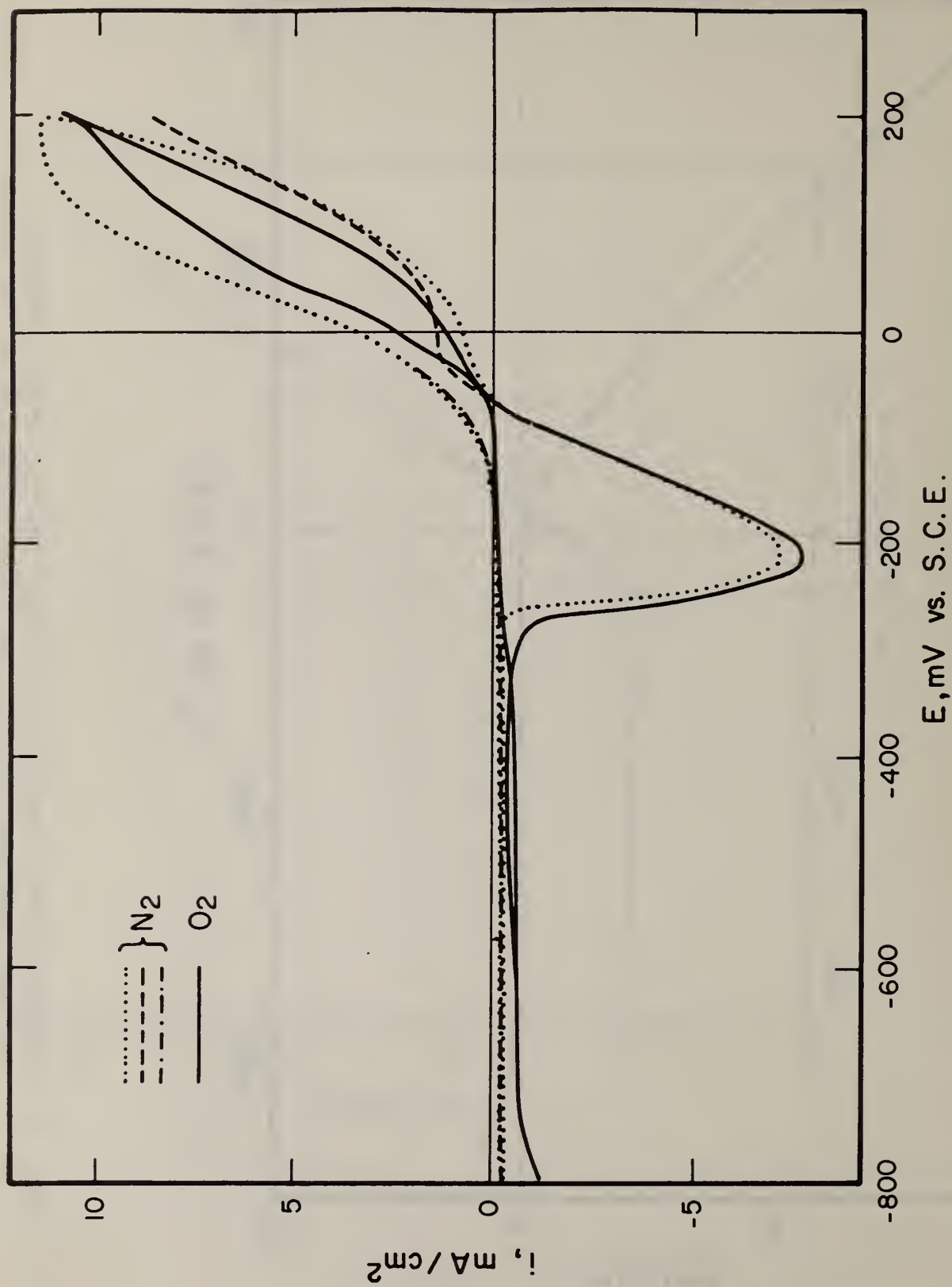


Fig. 22. Potentiodynamic scans for Cu in 2%  $\text{H}_2\text{SO}_4$  + 1%  $\text{NaCl}$ . Scan rate 4 mV/sec.

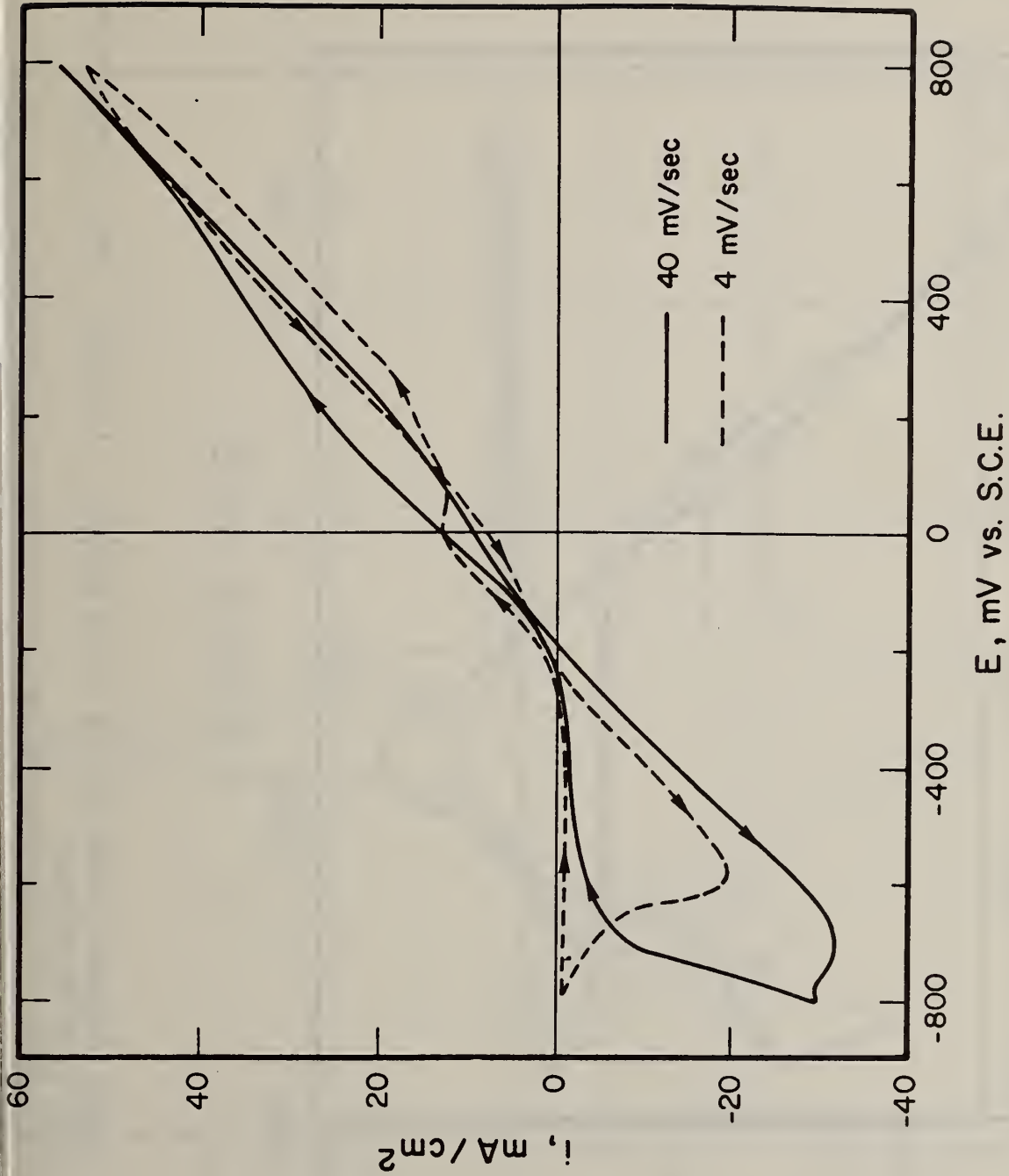


Fig. 23. Potentiodynamic scans for Cu in  $2.0 \text{ M H}_2\text{SO}_4 + 1\% \text{ NaCl}$ . Inert atmosphere.

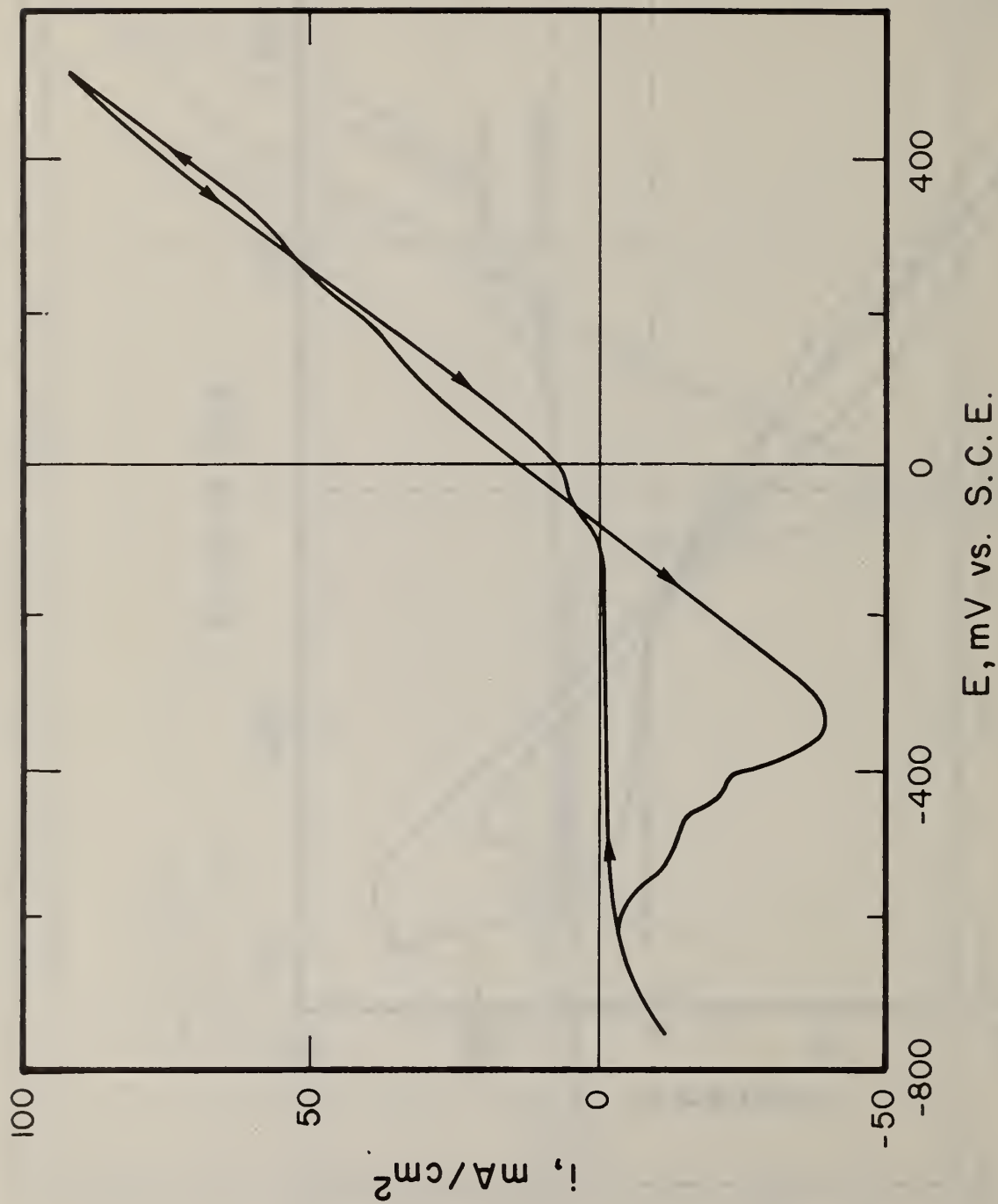


Fig. 24. Potentiodynamic scan for Cu in 2%  $\text{Na}_2\text{SO}_4$  + 1% NaCl. Inert atmosphere. Scan rate 40 mV/sec.

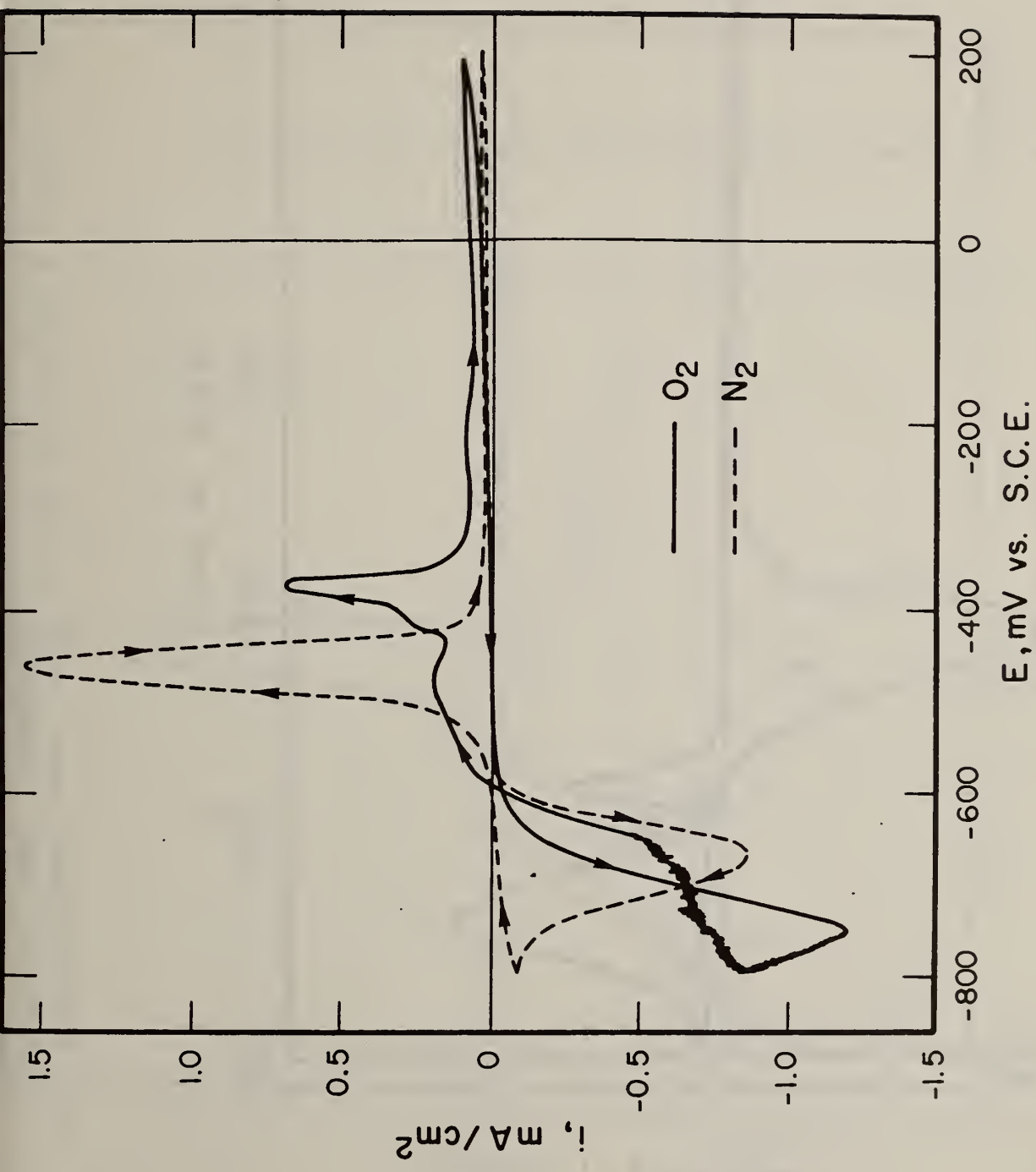


Fig. 25. Potentiodynamic scans for Pb-Sn alloy in 2M H<sub>2</sub>SO<sub>4</sub>. Scan rate 4 mV/sec.

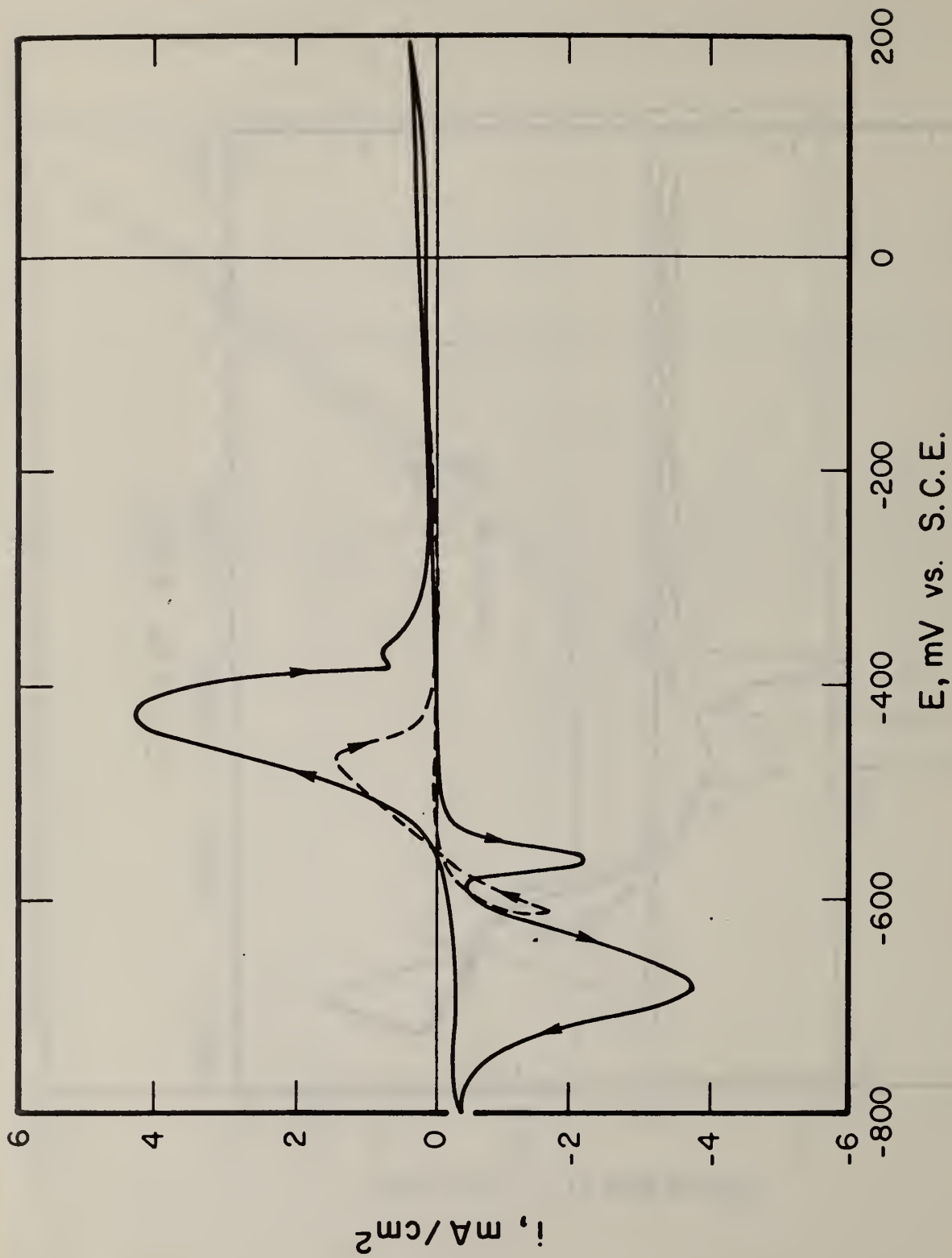


Fig. 26. Potentiodynamic scans for Pb-Sn alloy in 2%  $\text{H}_2\text{SO}_4$  + 1%  $\text{NaCl}$ . Scan rate 4 mV/sec. Inert atmosphere.

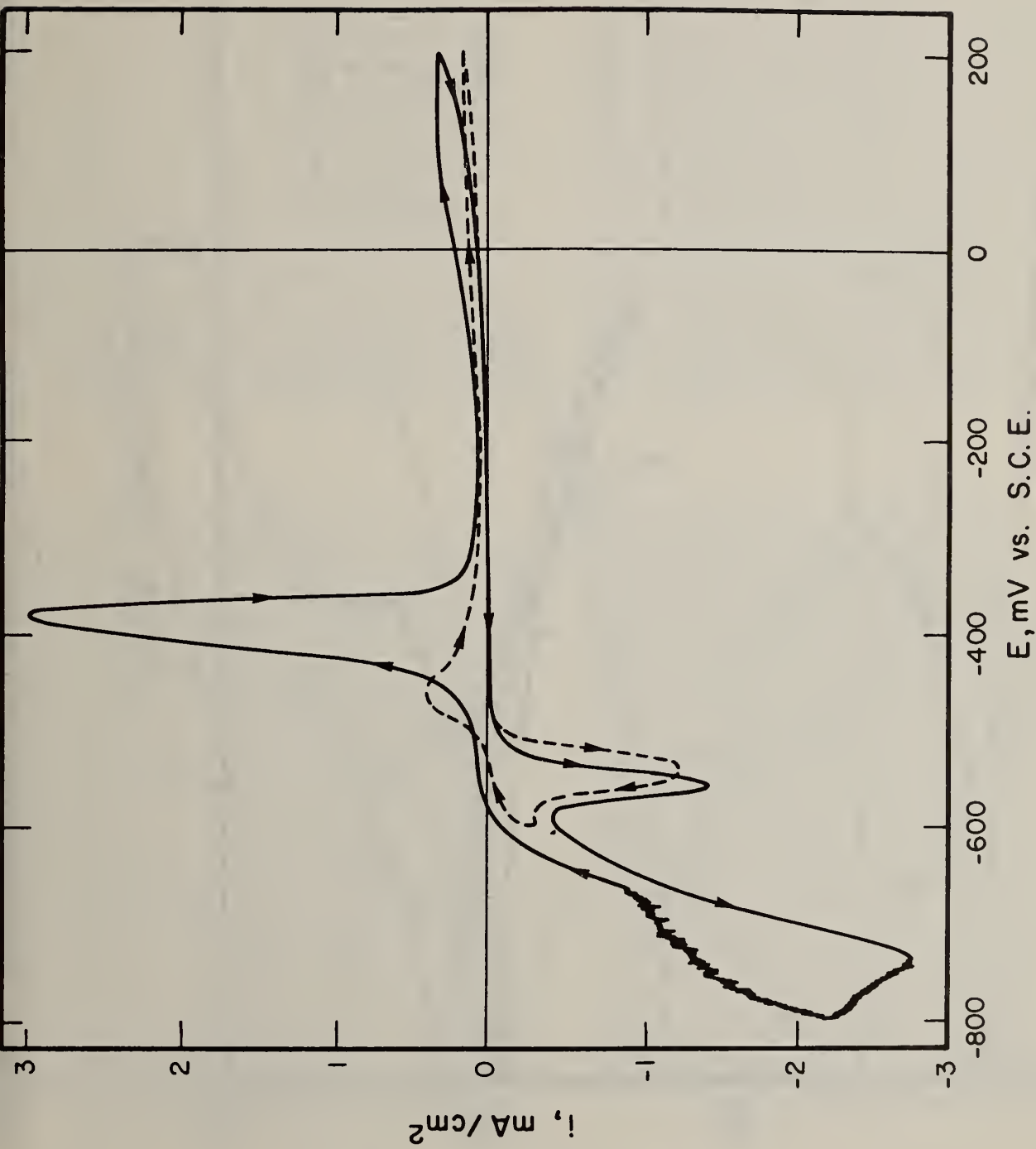


Fig. 27. Potentiodynamic scans for Pb-Sn alloy in 2%  $\text{H}_2\text{SO}_4$  + 1%  $\text{NaCl}$ . Oxygen atmosphere. Scan rate 4 mV/sec.

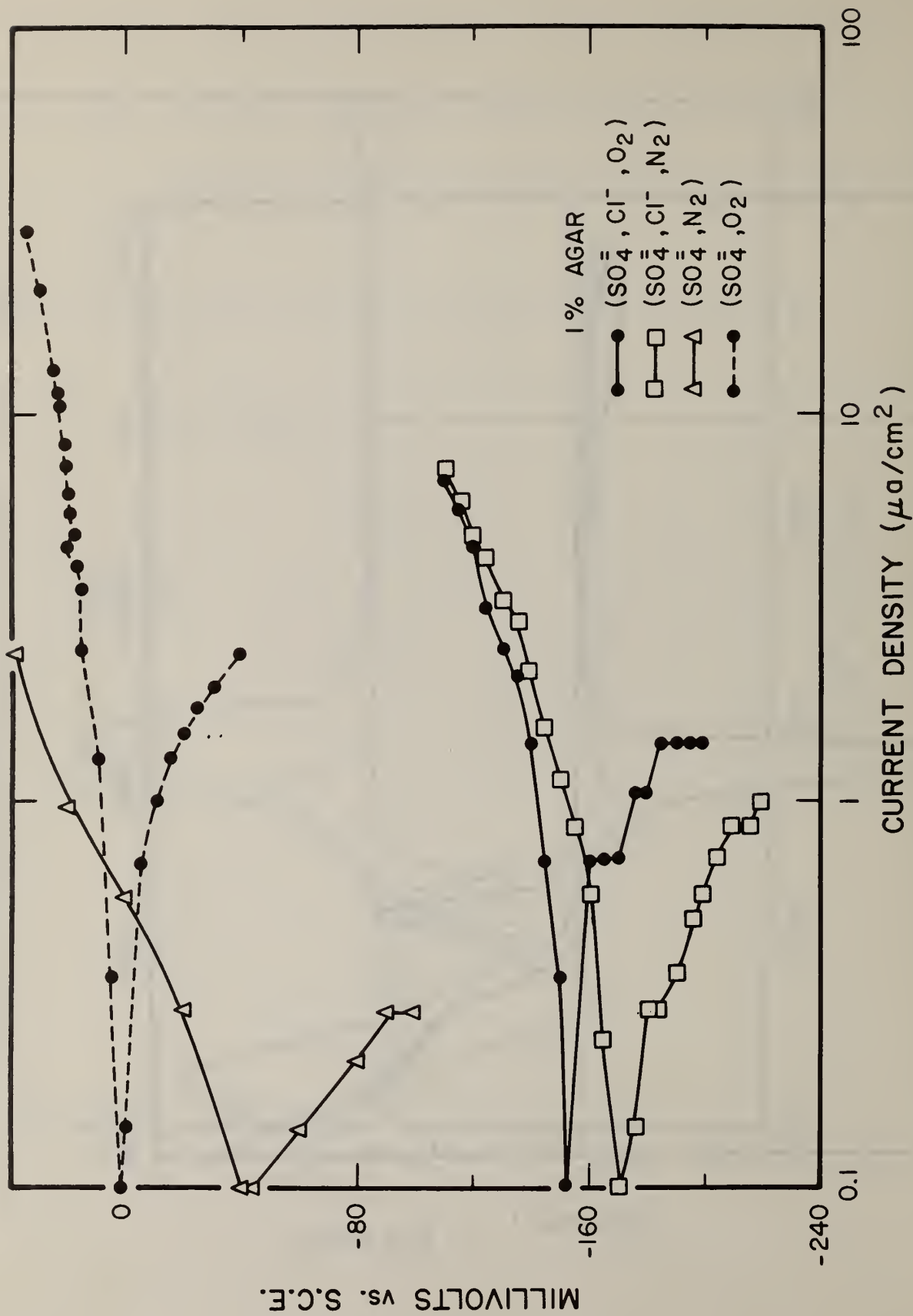


Fig. 28. Polarization curves for tinned Cu wire in 2% Na<sub>2</sub>SO<sub>4</sub>, taken in December 1976.

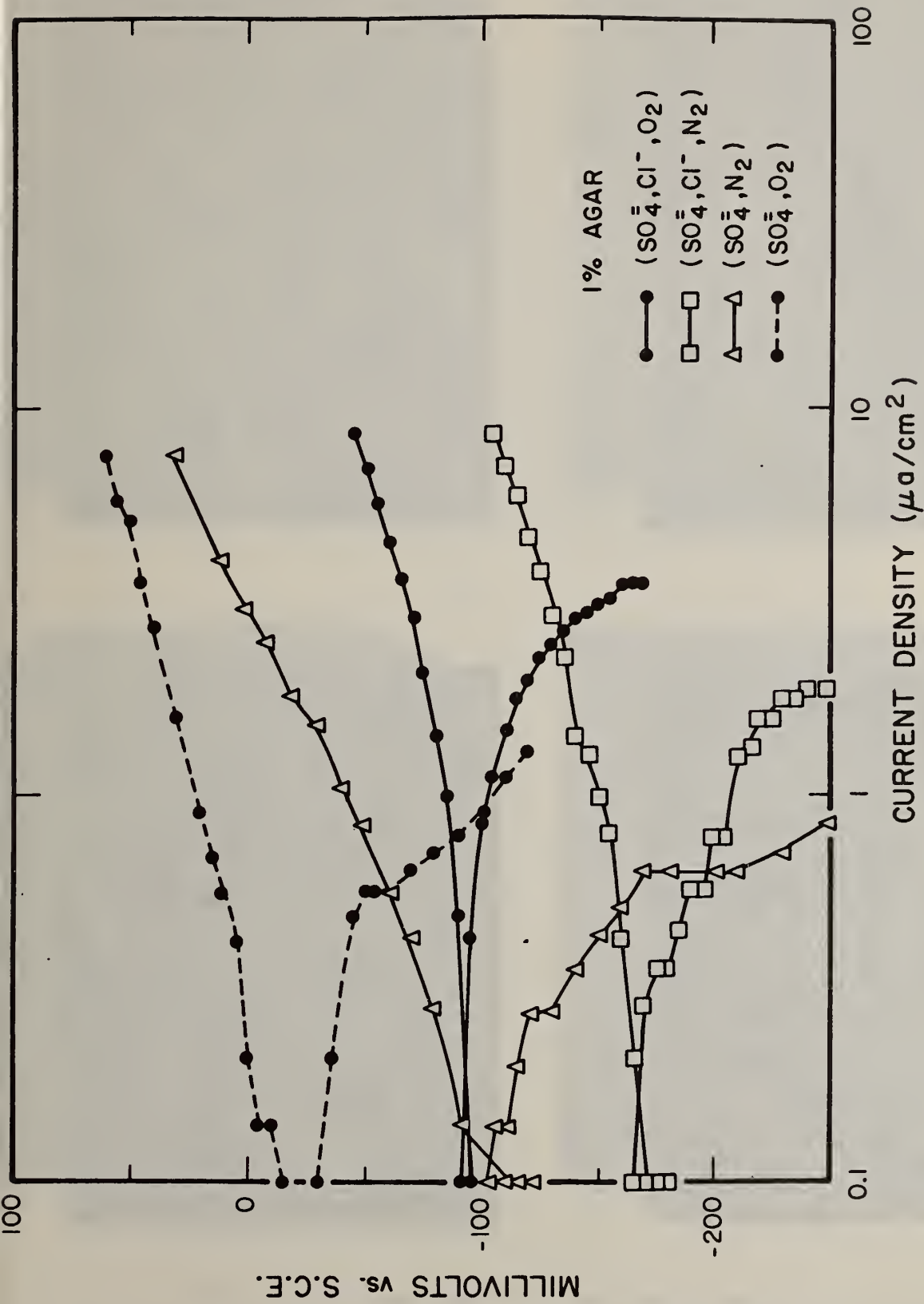
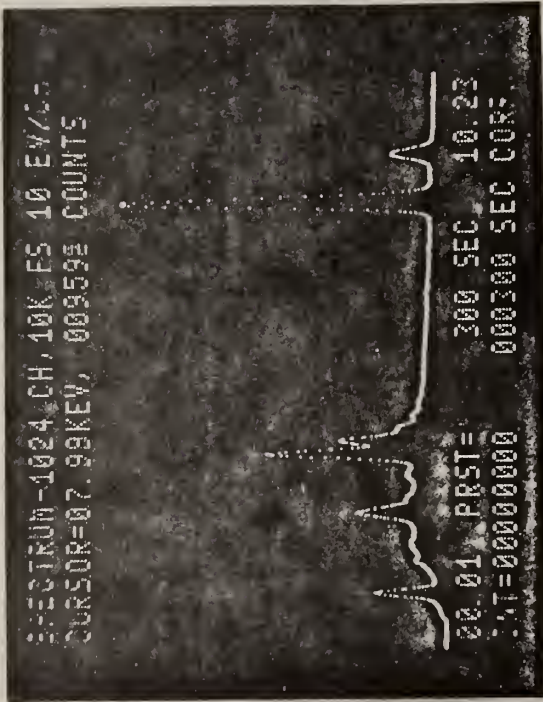
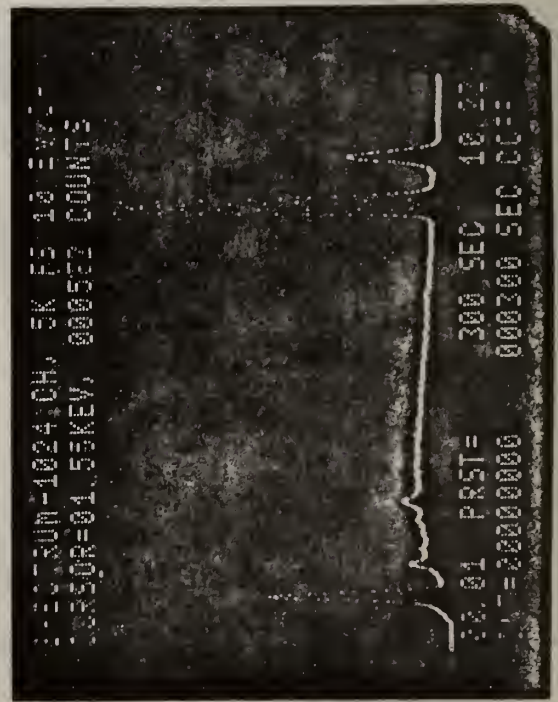


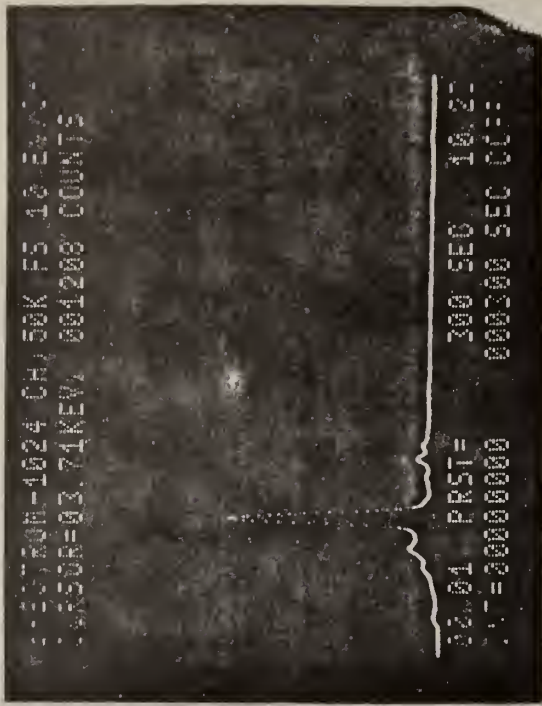
Fig. 29. Polarization curves for tinned Cu wire in 2%  $\text{H}_2\text{SO}_4$ , taken in January 1977.



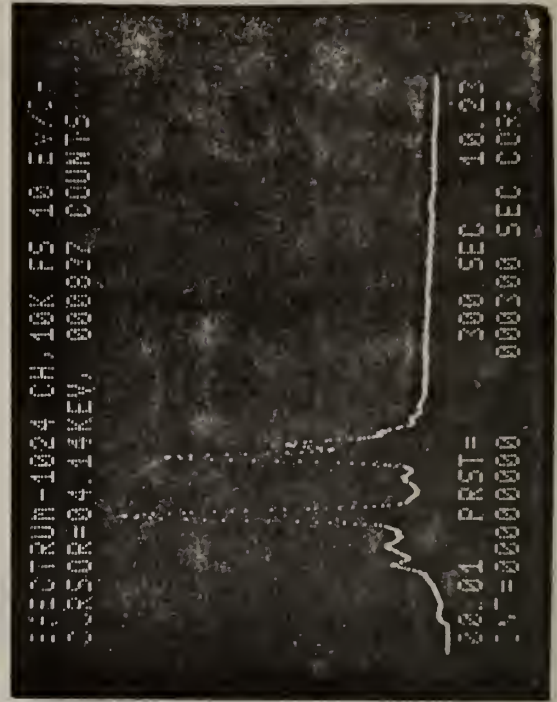
a) Concentric neutral wire as received



c) Pure copper wire

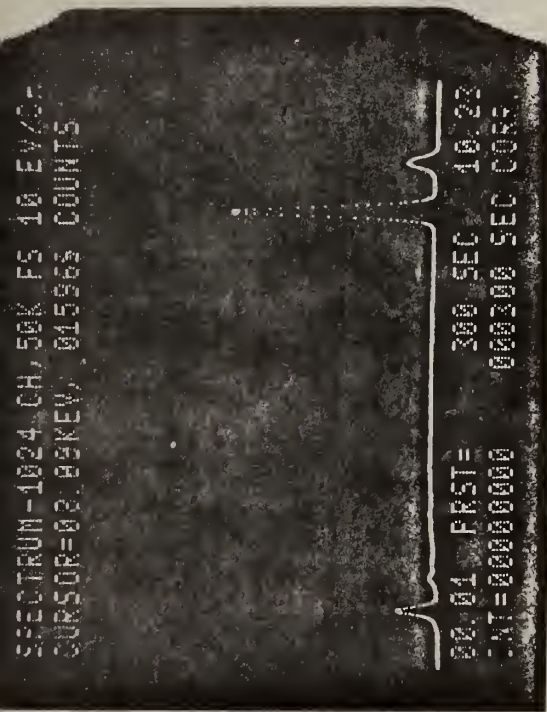


b) 90% Pb- 10% Sn alloy

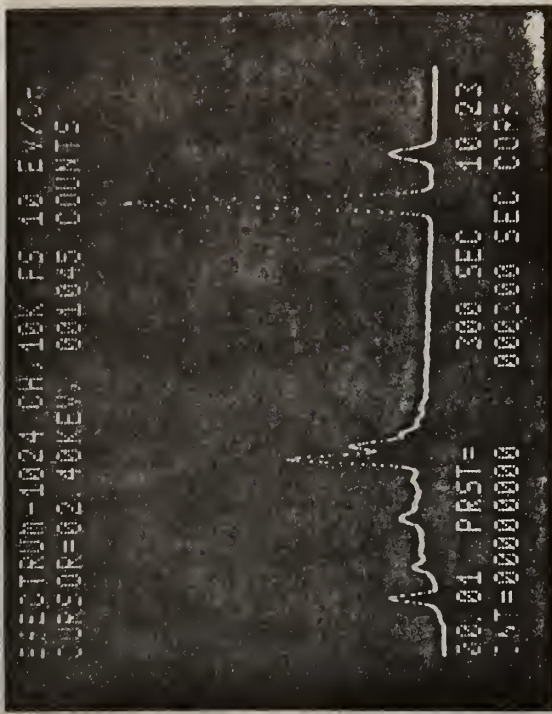


d) 60% Sn- 40% Pb alloy

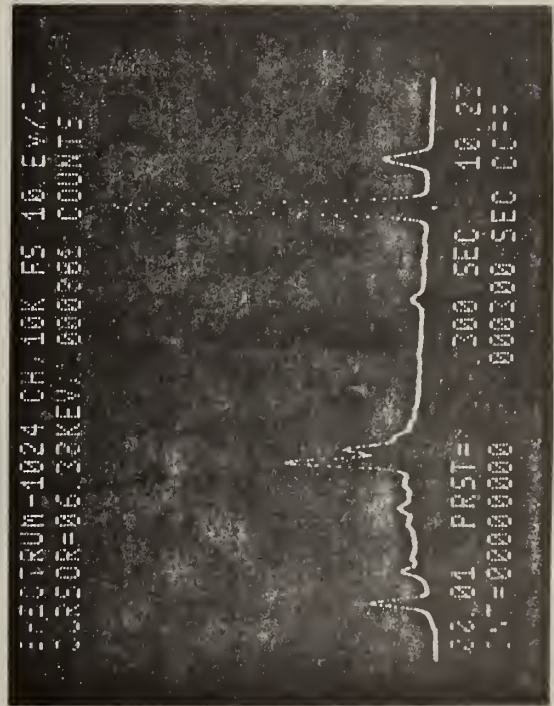
Fig. 30. X-ray spectra of various control specimens.



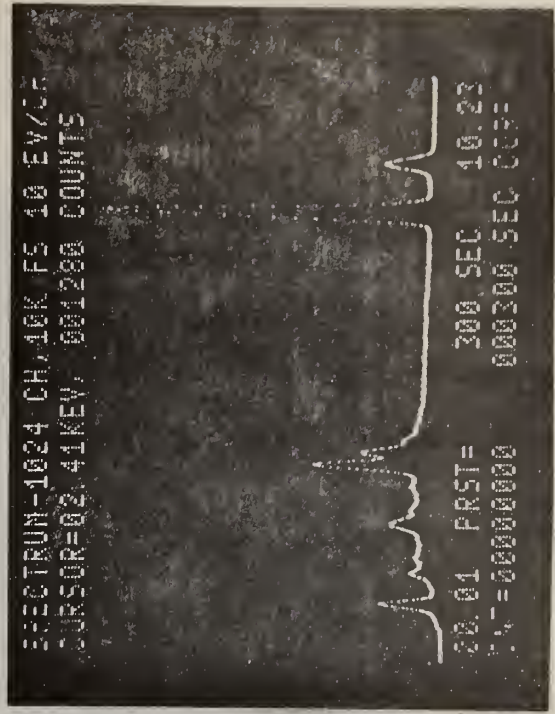
a) # 1.  $\text{H}_2\text{SO}_4 + \text{HCl}$ .  $\text{H}_2$ . a.c. 2100 h.



b) #101.  $\text{H}_2\text{SO}_4$ .  $\text{H}_2$ . 2200 h.

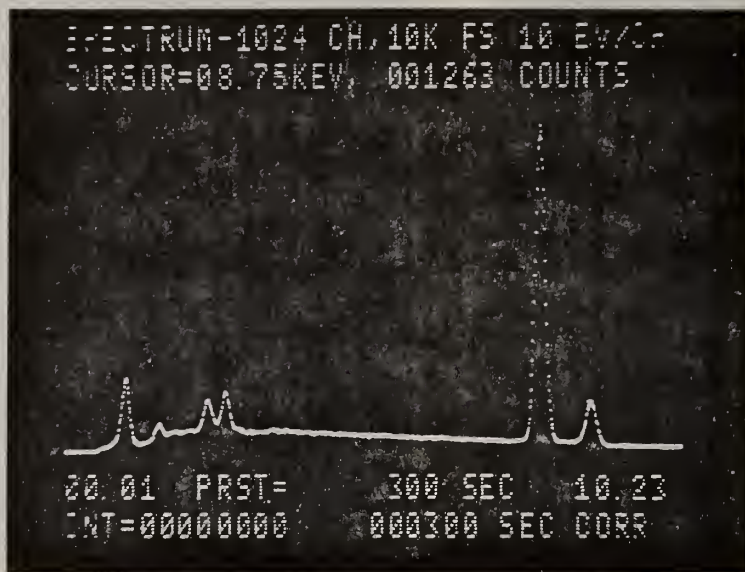


c) # 5.  $\text{H}_2\text{SO}_4 + \text{HCl}$ .  $\text{H}_2$ . a.c. CPE. 1700 h.



d) #104.  $\text{H}_2\text{SO}_4 + \text{HCl}$ .  $\text{H}_2$ . 2900 h.

Fig. 31. X-ray spectra of corroded neutral wires.



#119

Fig. 32. X-ray spectrum of corroded neutral wire. Solution  $\text{Na}_2\text{SO}_4 + \text{NaCl}$ .  $\text{O}_2$  atmosphere. CPE coupling. Agar. 1600 h.

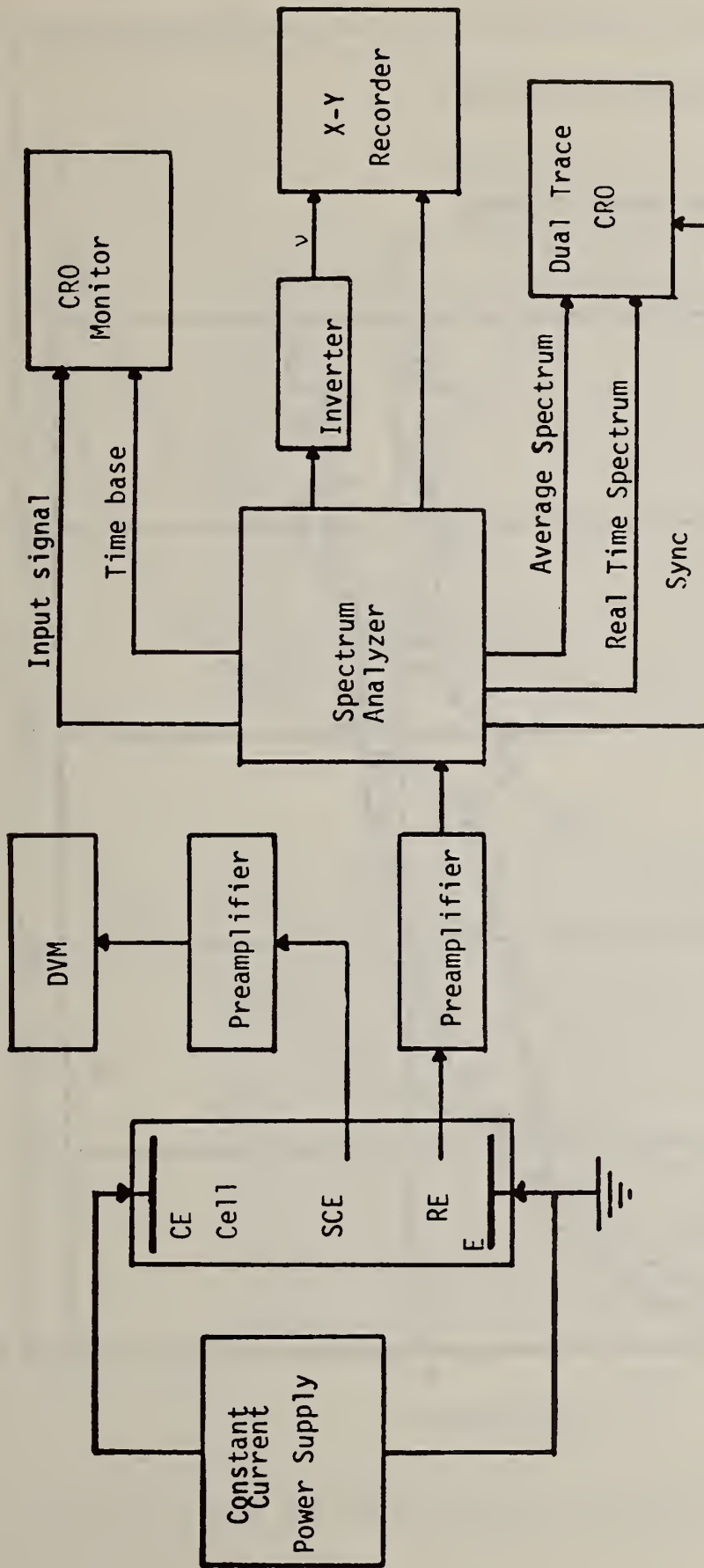


Fig.33. Schematic circuit for noise measurements.

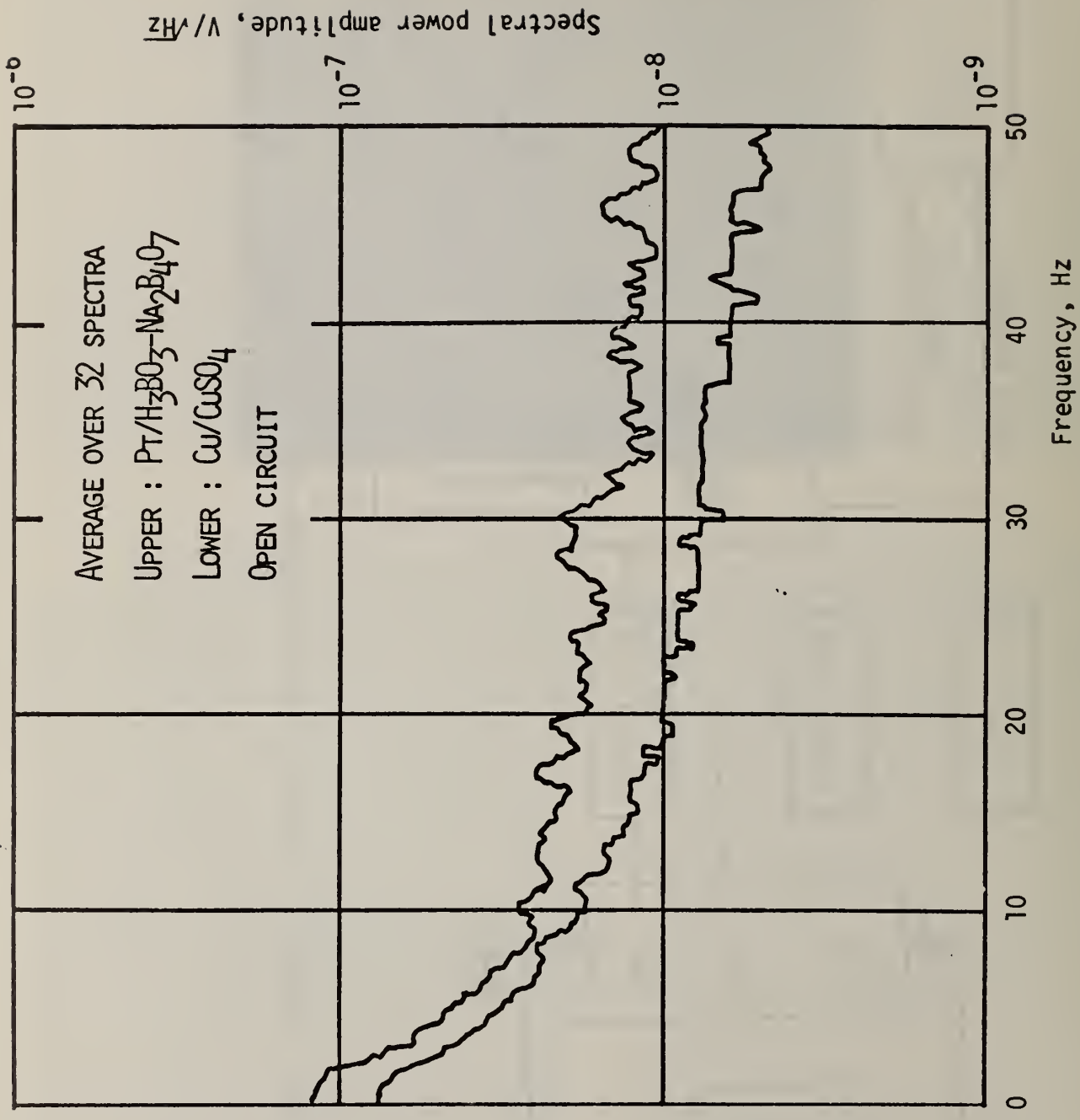


Fig.34. Noise spectrum at open circuit.

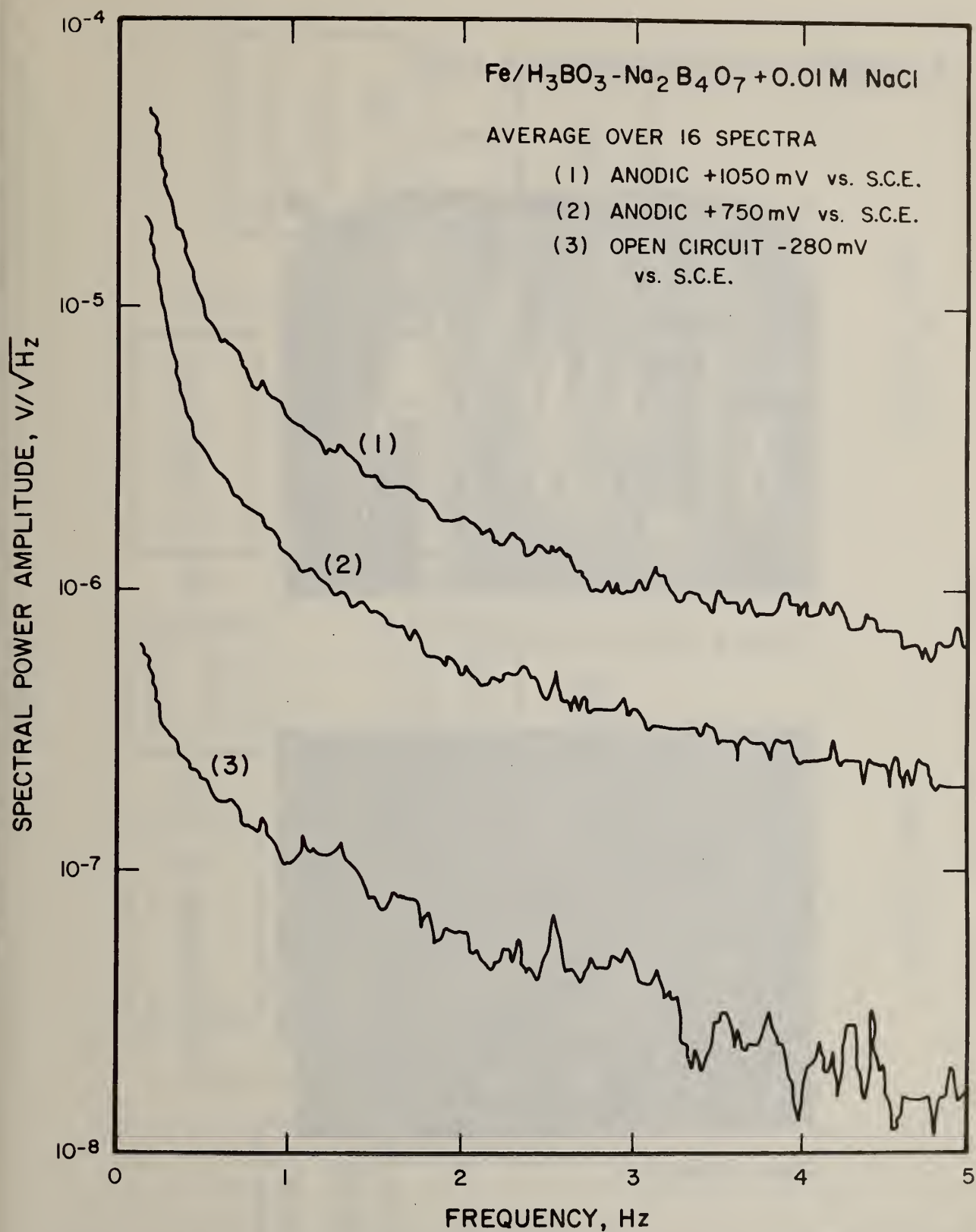
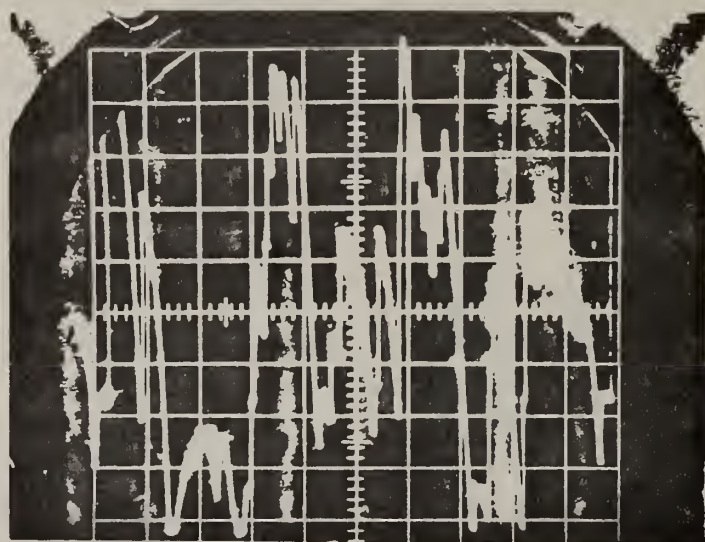


Fig. 35. Noise spectra of Fe in 1:1  $\text{H}_3\text{BO}_3\text{-Na}_2\text{B}_4\text{O}_7 + 0.01\text{ M NaCl}$  at various potentials.

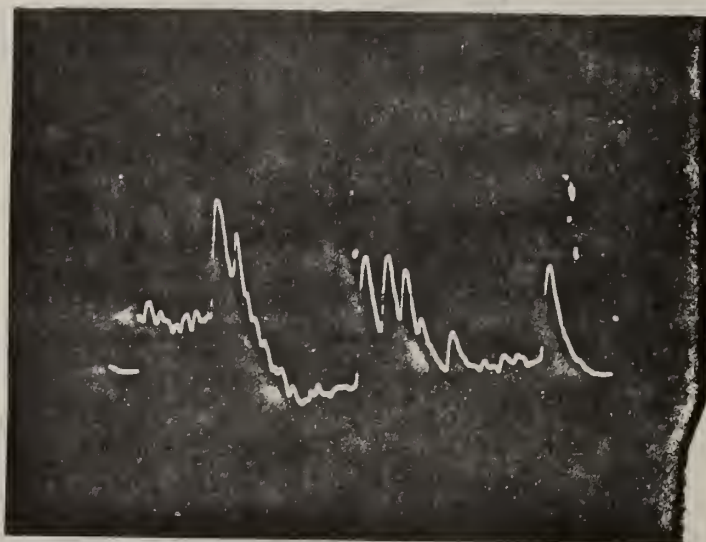
Fe/H<sub>3</sub>BO<sub>3</sub>-Na<sub>2</sub>B<sub>4</sub>O<sub>7</sub>+0.01 m NaCl

6.25·10<sup>-5</sup> V/DIV.



**Above Pitting Potential**

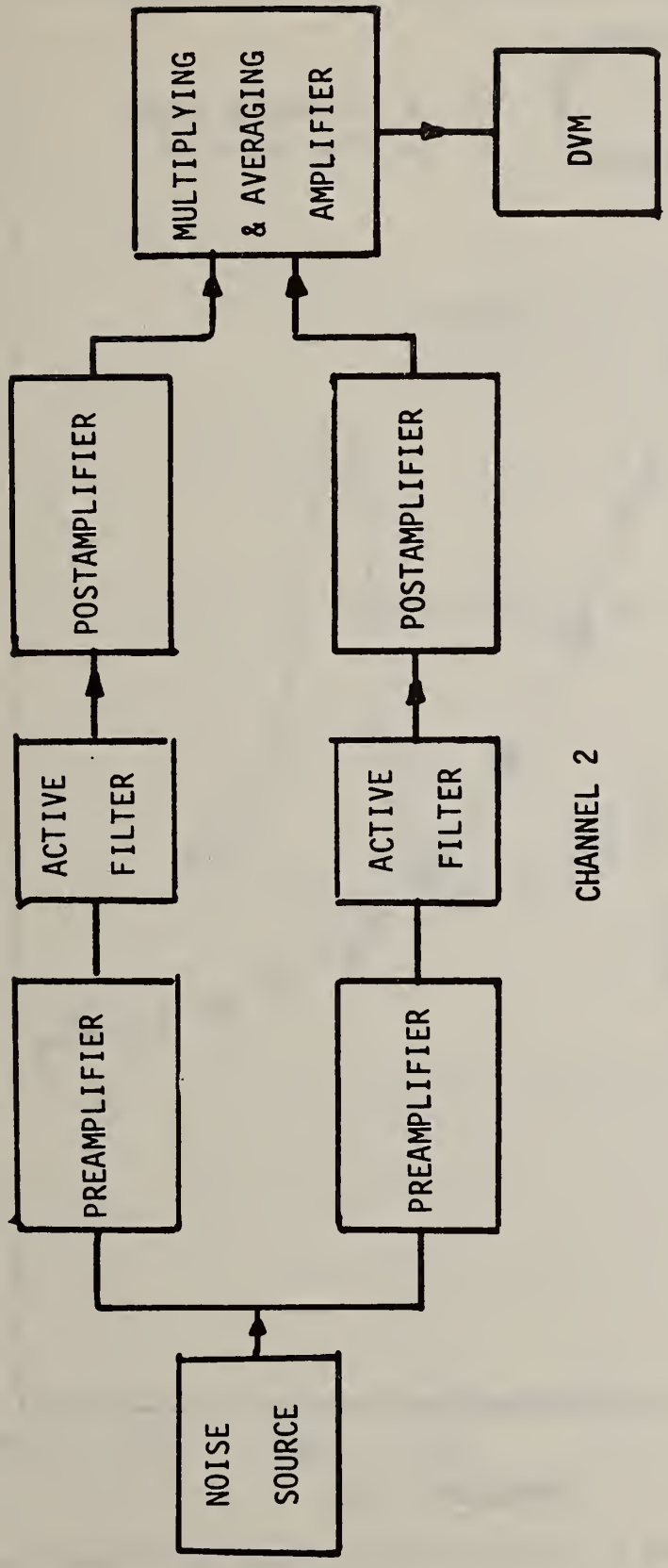
6.25·10<sup>-6</sup> V/DIV.



**Open Circuit**

Fig. 36. Oscillographic record of electrode potential of Fe in 1:1 H<sub>3</sub>BO<sub>3</sub>-Na<sub>2</sub>B<sub>4</sub>O<sub>7</sub>+0.01 m NaCl above and below the pitting potential.

CHANNEL 1



CHANNEL 2

Fig.37. Noise measuring circuit.

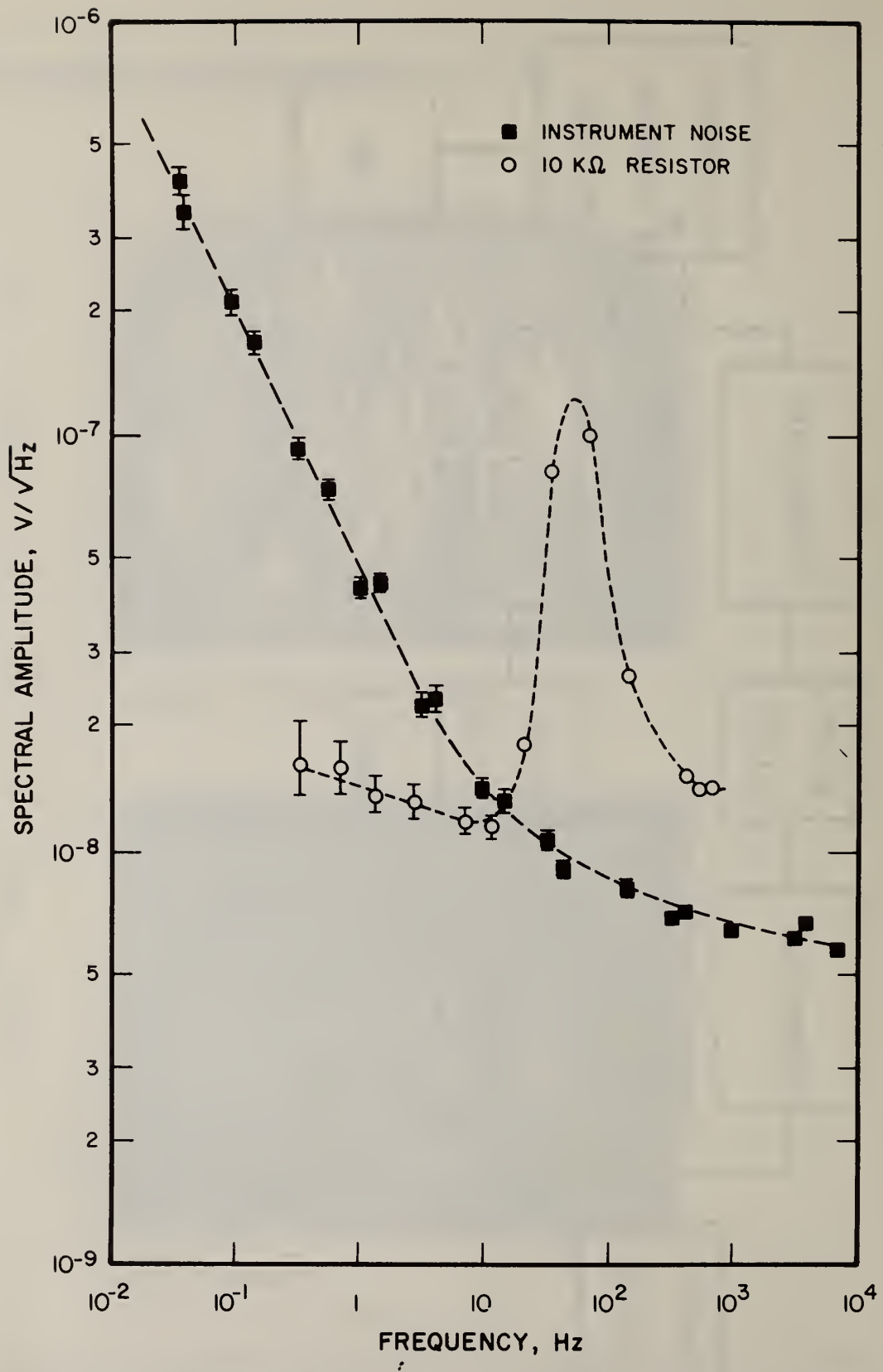
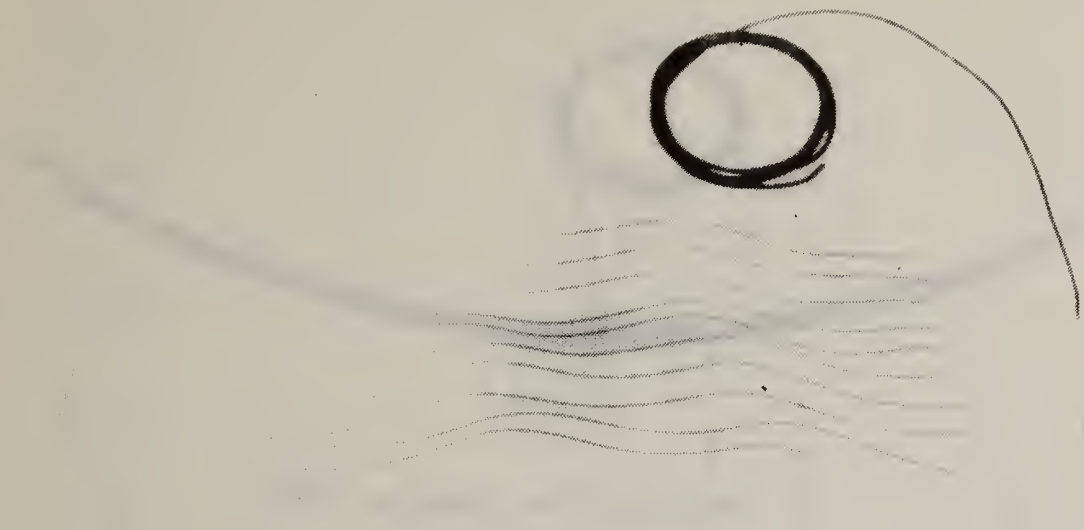
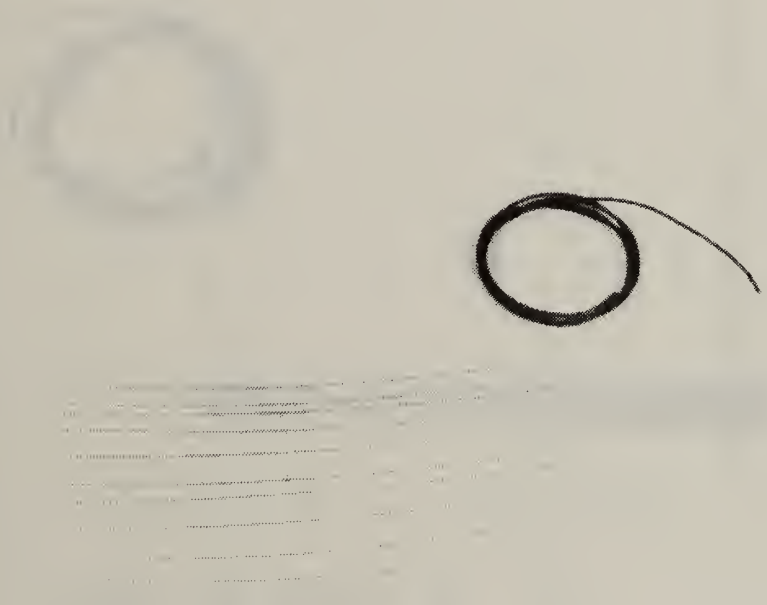


Fig. 38. Spectral power amplitude vs. frequency. Noise generated by the instrumentation and by a 10 k $\Omega$  resistor.

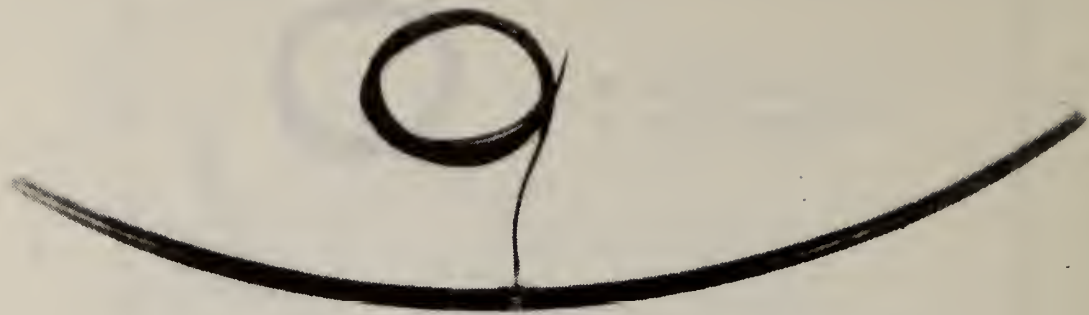


A) COATED COPPER WIRE

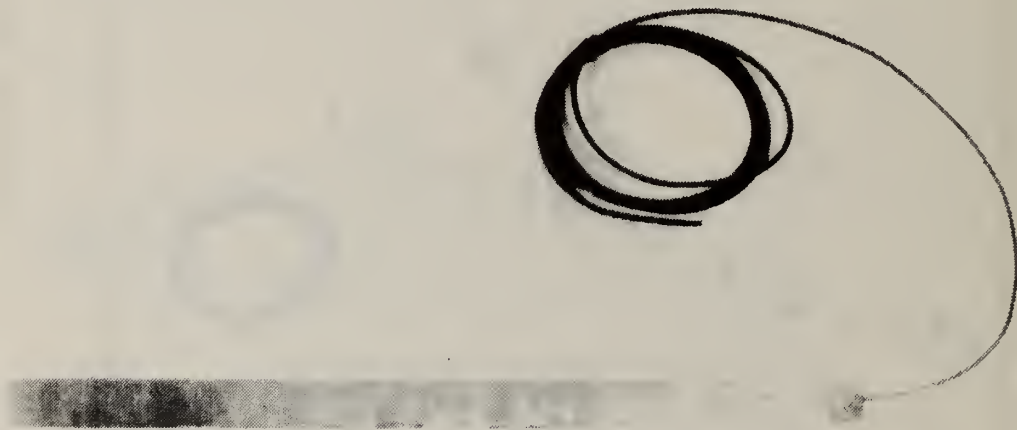


B) BARE COPPER WIRE

FIGURE 39

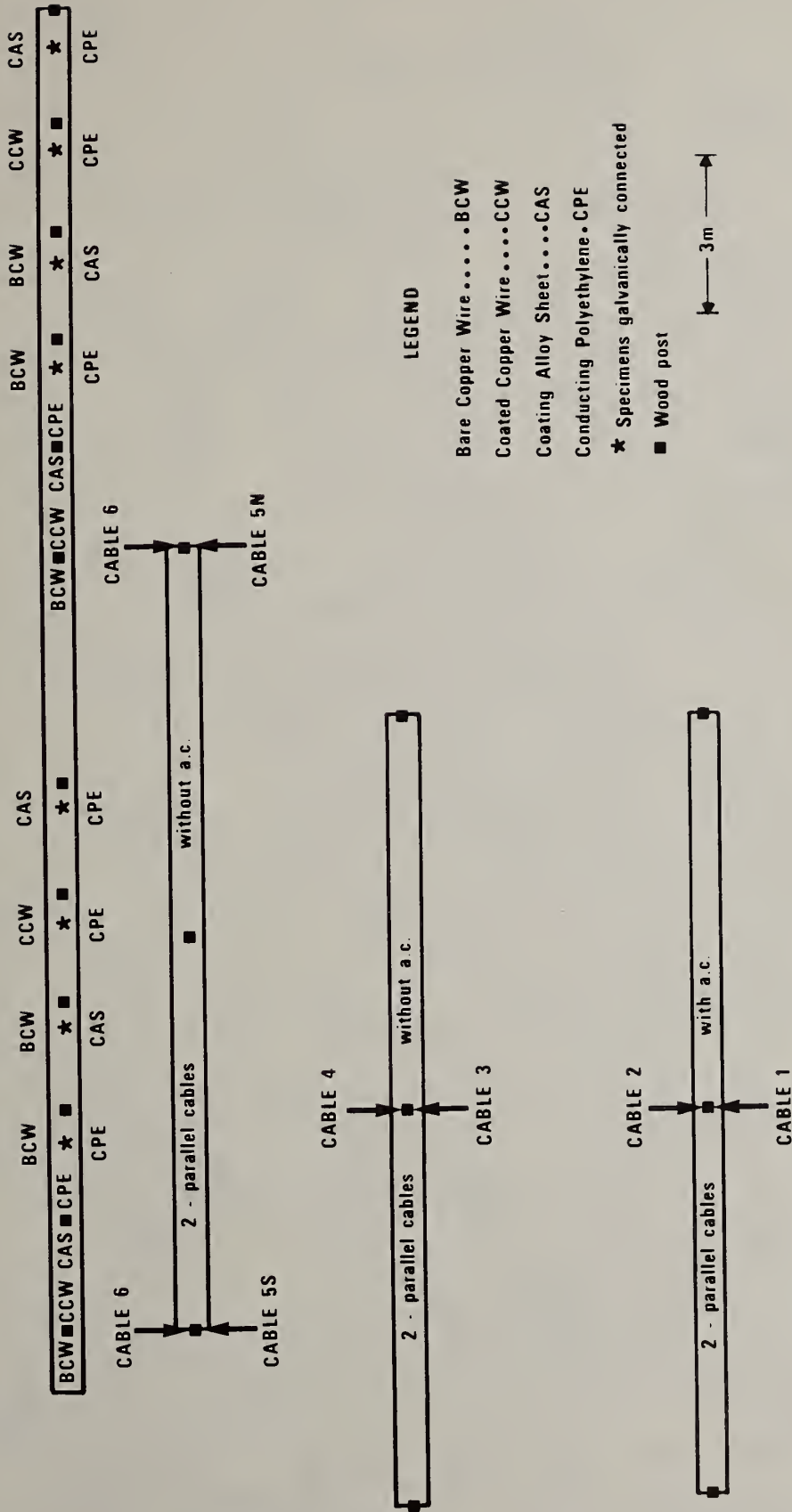


A) CONDUCTING POLYETHYLENE (CPE)



B) COATING ALLOY SHEET

FIGURE 40



NBS UNDERGROUND CORROSION TEST SITE

Fig 41

U.S. DEPT. OF COMM. BIBLIOGRAPHIC DATA SHEET	1. PUBLICATION OR REPORT NO. NBSIR 77-1232 (ERDA)	2. Gov't Accession No.	3. Recipient's Accession No.
4. TITLE AND SUBTITLE Development of IN-SITU Techniques for the Detection and Measurement of Corrosion of Copper Concentric Neutrals in Underground Environments		5. Publication Date	6. Performing Organization Code
7. AUTHOR(S) J. Kruger, U. Bertocci, F. Escalante, and J.L. Mullen		8. Performing Organ. Report No.	
9. PERFORMING ORGANIZATION NAME AND ADDRESS  NATIONAL BUREAU OF STANDARDS DEPARTMENT OF COMMERCE WASHINGTON, D.C. 20234		10. Project/Task/Work Unit No. 3120442	11. Contract/Grant No. E(49-1)-3800
12. Sponsoring Organization Name and Complete Address (Street, City, State, ZIP) Energy Research and Development Administration Washington, D.C. 20545		13. Type of Report & Period Covered Annual Report 1/15/76-1/15/77	14. Sponsoring Agency Code
15. SUPPLEMENTARY NOTES			
<p>16. ABSTRACT (A 200-word or less factual summary of most significant information. If document includes a significant bibliography or literature survey, mention it here.)</p> <p>The report describes the work done on the first year of a three-year project, whose purpose is to develop in-situ methods for detecting corrosion on buried copper concentric neutral (CCN) wires.</p> <p>Specimens of the wire underwent long term corrosion tests. Environmental variables examined were: a) composition of electrolyte, b) composition of the gaseous atmosphere, c) convective motion in solution, d) superimposed a.c. signal, and e) coupling with conducting polyethylene (CPE).</p> <p>The results showed that accelerated attack with pit formation was caused by a.c. signal and that oxygen availability and presence of chloride ions in solution favored the attack of the wires.</p> <p>Potentiodynamic scans on the wires as well as on pure copper and tinning alloy were performed in various solutions.</p> <p>The development of a new measurement method, the analysis of the fluctuations of the corrosion potential, has been initiated in the laboratory with the aim of testing its potentiality as a corrosion detection method in the field. A burial site on NBS grounds has been prepared, and several lengths of cable as well as some other pertinent materials have been laid underground. Data collection from the buried specimens has been initiated.</p>			
<p>17. KEY WORDS (six to twelve entries; alphabetical order; capitalize only the first letter of the first key word unless a proper name; separated by semicolons)</p> <p>Buried cables; copper concentric neutral wires; corrosion detection methods; corrosion tests; current-potential measurements; underground corrosion</p>			
<p>18. AVAILABILITY</p> <p><input checked="" type="checkbox"/> Unlimited</p> <p><input type="checkbox"/> For Official Distribution. Do Not Release to NTIS</p> <p><input type="checkbox"/> Order From Sup. of Doc., U.S. Government Printing Office Washington, D.C. 20402, SD Cat. No. C13</p> <p><input checked="" type="checkbox"/> Order From National Technical Information Service (NTIS) Springfield, Virginia 22151</p>	<p>19. SECURITY CLASS (THIS REPORT)</p> <p>UNCLASSIFIED</p> <p>20. SECURITY CLASS (THIS PAGE)</p> <p>UNCLASSIFIED</p>	<p>21. NO. OF PAGES</p> <p>69</p> <p>22. Price</p> <p>\$4.50</p>	